CHAPTER 20

NETWORK THEORIES FOR POLYMER MELTS AND CONCENTRATED SOLUTIONS[1]

Most of this volume has focused on molecular theories of dilute solutions in which polymer–polymer interactions are neglected. All dilute solution theories predict that the viscosity should depend linearly on the polymer concentration. However, we know that the range in which the dilute solution assumption applies is limited to very small concentrations. At larger concentrations the zero-shear-rate viscosity increases much faster than linearly with concentration, indicating strong polymer–polymer interactions (see Eq. 3.6-15). The approach to the molecular description of concentrated solutions and melts taken in the previous chapter was to construct a systematic application of the general phase-space kinetic theory which included the interaction between two or more polymer molecules. There the polymer–polymer interactions were accounted for primarily by taking into account the constraints imposed on the motion of a polymer molecule resulting from the close proximity of the neighboring molecules. This is accomplished by requiring that Brownian motion be highly anisotropic ("reptation") and that the hydrodynamic drag on the beads also be anisotropic.

Here we take a different approach in modeling the interactions of the polymer molecules which builds on the classical network theories of rubber elasticity. In the network theories of macromolecular solids, chemical crosslinks are described as points, or junctions, at which connecting portions of molecules are forced to move together for all times. In adapting this theory to liquids we assume the junctions are not permanent, but are continually being created and destroyed. However, we apply the central idea from the solid theory and assert that polymer–polymer interactions are described by the temporary cooperative movement of molecular segments joined by these transient "crosslinks."

The theoretical development of the network theory is much simpler than that for the phase-space treatment in Chapter 19. The primary deficiency of the network approach taken here is that it does not provide the molecular description of the central process of junction formation and destruction. This means that the relaxation spectrum is not given explicitly by the theory in terms of molecular model parameters as was the case for the

[1] The authors are greatly indebted to Professor Arthur S. Lodge of the University of Wisconsin–Madison in connection with the preparation of this chapter. We have made considerable use of his research papers, unpublished lecture notes, and informal comments. The approach taken in this chapter is patterned after A. S. Lodge, R. C. Armstrong, M. H. Wagner, and H. H. Winter, *Pure Appl. Chem.*, **54**, 1349–1359 (1982).

For other general treatments of network theories see M. Yamamoto, *J. Phys. Soc. Japan*, **11**, 413–421 (1956); **12**, 1148–1158 (1957); **13**, 1200–1211 (1958); F. W. Wiegel, *Physica*, **42**, 156–164 (1969); F. W. Wiegel and F. Th. de Bats, *Physica*, **43**, 33–44 (1969).

phase-space theory. However, the constitutive equations obtained from the network theory are much simpler to use than the corresponding Chapter 19 results.

In the first section we introduce the terminology that is needed to describe the network models. Then in the next section we develop a balance equation for network segments, which allows us to describe the "configuration" of a polymer network undergoing flow. Then in §20.3, we derive an expression for the stress tensor in terms of the configuration of the network. It should be noted that §§20.2 and 3 are very similar to §§13.2 and 3 as to scope and general procedures. §§20.4 and 5 specialize the general network theory results to several models that have been studied extensively in the literature and to some new models which appear to be particularly promising.

§20.1 DESCRIPTIONS OF NETWORK MODELS

The central approximation in all network theories of macromolecular materials is that polymer–polymer interactions are localized at *junctions*. A junction is a strong local attraction between isolated points along two different polymer chains at which the interacting points are constrained to coincide. In macromolecular solids, the junction is the point at which there is a permanent *chemical* crosslink; in macromolecular fluids, junctions are temporary *physical* entanglements of various complexities and lifetimes. The macromolecular chain joining two successive junctions is called a network *segment*. A macromolecular chain which is connected to a junction at only one point is called a *loose end*, and a macromolecule not attached to the network is known as a *stray chain*. The totality of network segments is referred to as a molecular *network*, and *connectivity* is used to describe the organization of junctions tying the network together. A solid, crosslinked polymer is said to have constant connectivity, whereas a concentrated polymer solution or melt is said to have time-dependent connectivity.

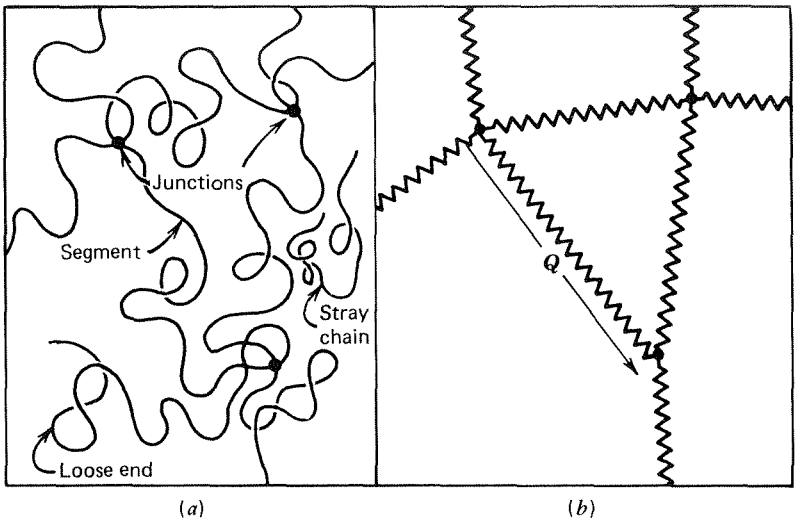

FIGURE 20.1-1. Small element of a macromolecular network. In (*a*) the "actual" molecular structure is shown; a segment, several junctions, a loose end, and a stray chain are labeled. The junctions could be either permanent crosslinks or temporary physical entanglements; the segments are composed of parts of macromolecules undergoing thermal motions. The statistical treatment of the system of part (*a*) replaces it by the classical system with Hookean springs shown in part (*b*). Part (*b*) also shows the segment vector $\boldsymbol{Q}$. Note that the loose end and stray chain of (*a*) are omitted from (*b*).

The definitions given above are illustrated in Fig. 20.1-1 which shows the idealization made in treating polymeric materials as networks. All polymeric chains that are not network segments, that is, all loose ends and stray chains are entirely neglected in the network theory. For example, the loose end and stray chain in Fig. 20.1-1(a) have no representation in the idealized network of Fig. 20.1-1(b).

The following six assumptions are common to network theories for both solids and liquids:

i. A concentrated polymer solution, polymer melt or crosslinked polymeric solid can be represented by a molecular network with polymer–polymer interactions occurring only as strong local interactions at isolated points along the chains. This network is *coherent* in the sense that each network point is connected by at least two continuous network paths to the bounding surface of a physically infinitesimal material element. This network alone is responsible for the rheological behavior of the material; loose ends and stray chains are neglected.

ii. The polymeric material is assumed to be incompressible, that is, we consider only deformations at constant volume.[2]

iii. The network junction points move *affinely*,[3] that is, as if they were material particles in an equivalent macroscopic continuum. The thermal motions of the junctions are neglected.

iv. The phase space distribution function for each segment is equilibrated at all times.

v. The polymeric material is subjected to either a homogeneous deformation or a homogeneous flow.

vi. Each network segment can be modeled as a *Gaussian* chain.[4] We take the segments to be freely jointed, bead-rod chains, in which the end-to-end distance of any segment is small compared with $a(N-1)$, where $N-1$ is the number of rods in the segment and a is the length of each rod. Together with assumption (iv) above this means that each segment can be modeled as a Hookean spring with spring constant $H_N = 3kT/(N-1)a^2$ (cf. Eq. 11.3-20).

Except as noted above, these assumptions may not be removed without fundamental changes in the theory. The network theory for solids rests essentially upon these assumptions with only very minor additional assumptions. The strikingly good agreement[5] between the predictions of the network theory for solids and experimental observations indicates that assumptions (i) to (vi) are valid for materials such as crosslinked rubber. It is not yet clear whether these same assumptions are equally valid for polymeric fluids.

For fluids we make the following additional assumptions:

vii. Segments are lost and created during flow. At any one time, the network will therefore consist of segments with a distribution of ages. The stress is assumed to be the sum of contributions from all segments existing at the present time, these having been created at various past times.

[2] A. S. Lodge, *Proc. VII International Cong. Rheology*, C. Klason and J. Kubát, eds. (Gothenburg), 79–84 (1976), has extended the network theory to allow for compressibility.

[3] The implications of nonaffine junction motion are explored in §20.5. An alternative to assuming that each junction point moves affinely is given in H. M. James, *J. Chem. Phys.*, **15**, 651–668 (1947) where the concept of "boundary points" is introduced. These are points of the network segments where the segments intersect the surface of a volume element enclosing the system under investigation. Instead of the affine junction motion assumption, James merely assumes that the boundary points also move affinely; he then calculated the motion of the junctions, thereby formulating a theory somewhat more general than the one considered here. However, this extra generality in the formulation does not lead to a more general constitutive equation.

[4] The removal of the Gaussian assumption has been shown by A. S. Lodge, *Rheol. Acta*, **7**, 379–392 (1968) to give no substantial improvement in the constitutive equation for polymeric liquids.

[5] L. R. G. Treloar, *The Physics of Rubber Elasticity*, 3rd ed., Oxford University Press, London (1975).

viii. It is assumed that the distribution function for the network segments at the moment of creation is identical to the equilibrium distribution function for a freely jointed, bead-rod chain with no constraints on the end points. The Gaussian distribution for newly created segments is sometimes referred to as the "Wall distribution."

ix. Segments may be characterized by a single positive integer i that indicates the "complexity" of the segment.

For fluids not much is known about the mechanisms of formation and loss of the temporary entanglements. Thus the theory focuses instead on the segments. It is expected that many different kinds of physical entanglements can be formed and that these will exhibit a wide range of degree of permanence. The idea of *segment complexity* is used to describe the relative permanence of different segments. The origin of segment complexity is illustrated in Fig. 20.1-2 where segments formed as a result of temporary physical entanglements are contrasted with those formed between permanent chemical crosslinks. For the solid, segments are all of the same complexity, since they are all permanent. For the fluid, the complexity of a segment is tied to the topology of the "knot" that is formed by Brownian motion and which constitutes the junction. As shown in Fig. 20.1-1(b) the end-to-end vector for a typical segment is given by $\boldsymbol{Q}$.

We will henceforth refer to segments of type i which are composed of $N-1$ equivalent random links as iN-segments. We now introduce a distribution function $\Psi_{iN}(\boldsymbol{Q}, t)$ which is defined such that

$$\Psi_{iN}(\boldsymbol{Q}, t)d\boldsymbol{Q} = \text{number of segments per unit volume at time } t \text{ that have complexity } i \text{ and } N-1 \text{ equivalent random links and that have end-to-end vector in the range } d\boldsymbol{Q} \text{ about } \boldsymbol{Q}. \tag{20.1-1}$$

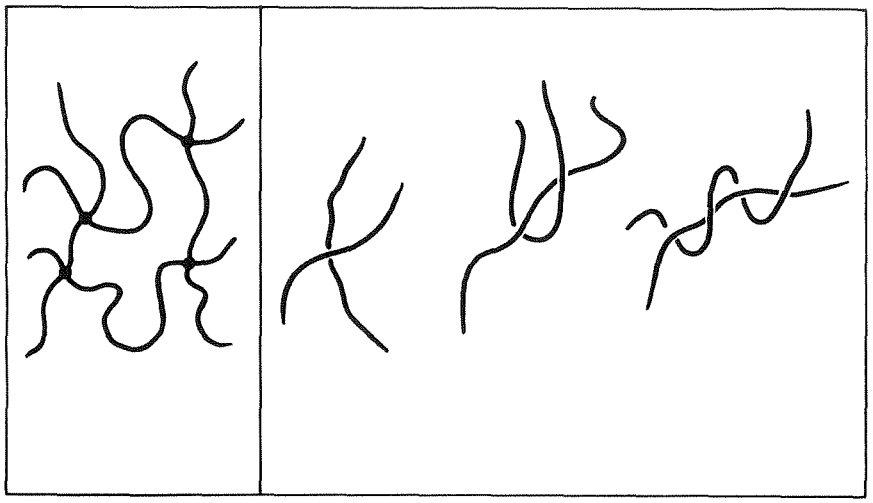

(*a*) (*b*)

FIGURE 20.1-2. Junctions in (*a*) macromolecular solids and (*b*) macromolecular network fluids. The junctions in (*a*) are chemical crosslinks and result in permanent segments. The junctions in (*b*) are physical entanglements and result in temporary segments. As illustrated in (*b*) many different types of entanglements can be formed by Brownian motion and these will differ in longevity. The variability in junction durability leads to segments of varying complexity.

The distribution function is normalized as follows:

$$\int \Psi_{iN}(\boldsymbol{Q}, t)d\boldsymbol{Q} = n_{iN} \tag{20.1-2}$$

in which n_{iN} is the number density of iN-segments. We assume n_{iN} is independent of position. The number density of all segments at any time is

$$n = \sum_N n_N = \sum_i \sum_N n_{iN} \tag{20.1-3}$$

where n_N is the number density of segments of all complexities that have $N - 1$ equivalent random links. It is also sometimes convenient to assume that Ψ_{iN} can be factored as follows:

$$\Psi_{iN}(\boldsymbol{Q}, t) = n_{iN}\psi_N(\boldsymbol{Q}, t) \tag{20.1-4}$$

where

$$\psi_N(\boldsymbol{Q}, t)d\boldsymbol{Q} = \text{probability that a segment with } N \text{ equivalent random links has an end-to-end vector between } \boldsymbol{Q} \text{ and } \boldsymbol{Q} + d\boldsymbol{Q} \tag{20.1-5}$$

depends only on N and not on the complexity of the segment. We require

$$\int \psi_N(\boldsymbol{Q}, t)d\boldsymbol{Q} = 1 \tag{20.1-6}$$

to be consistent with the normalization of Ψ_{iN}.

§20.2 CONVECTION EQUATION FOR NETWORK SEGMENTS

In this section we derive an equation that determines the distribution function for the segments. This equation is derived by a method similar to that used for obtaining the diffusion equation for elastic dumbbell models in §13.2. For network models, the equation of motion is much simpler than that for the elastic dumbbells, but the continuity equation for the network is slightly more complicated because of the creation and destruction terms for the segments.

a. The Equation of Motion for Network Segments

Since it is assumed that the junction points move affinely, it follows that the segment vector $\boldsymbol{Q}$ which joins two junctions must also move affinely. This gives the equation of motion for a segment

$$\dot{\boldsymbol{Q}} = [\boldsymbol{\kappa} \cdot \boldsymbol{Q}] \tag{20.2-1}$$

where $\dot{\boldsymbol{Q}} = d\boldsymbol{Q}/dt$. Equation 20.2-1 can be integrated to give an explicit expression for $\boldsymbol{Q}(t)$,

$$\boldsymbol{Q} = [\mathbf{E} \cdot \boldsymbol{Q}'] \tag{20.2-2}$$

in which we have used the initial condition that at $t = t'$, $\boldsymbol{Q} = \boldsymbol{Q}(t') = \boldsymbol{Q}'$. $\mathbf{E}(t, t')$ is the deformation gradient between times t' and t (cf. Eq. D.1-6, Eq. 9.2-5).

b. The Equation of Continuity for $\Psi_{iN}(\boldsymbol{Q}, t)$

The configuration of a single segment is given by specifying the three Cartesian coordinates X, Y, Z of its end-to-end vector $\boldsymbol{Q}$. For a concentrated polymer solution or melt containing many segments, the time rate of change of iN-segments in the volume $\Delta X \Delta Y \Delta Z$ in configuration space is

$$\frac{\partial}{\partial t} \Psi_{iN}(\boldsymbol{Q}, t) \Delta X \Delta Y \Delta Z \tag{20.2-3}$$

The net rate at which segments enter the given configuration volume because of the flow of the liquid is

$$(\dot{X}\Psi_{iN})|_X \Delta Y \Delta Z - (\dot{X}\Psi_{iN})|_{X+\Delta X} \Delta Y \Delta Z \tag{20.2-4}$$

$$+2 \text{ additional pairs of terms for the } Y \text{ and } Z \text{ directions.}$$

Finally, it is possible that segments are created and destroyed by the flow, because of the temporary nature of the junctions in liquid polymers. Let the number per unit volume of iN-segments of length Q that are created per unit time at time t be denoted by $L_{iN}(Q, t)$. Next let us denote the probability per unit time that an iN-segment will be destroyed as $\lambda_{iN}^{-1}(Q, t)$. Then for the configuration volume $\Delta X \Delta Y \Delta Z$ the rate at which iN-segments are created minus the rate of destruction is

$$\left(L_{iN}(Q, t) - \frac{\Psi_{iN}}{\lambda_{iN}(Q, t)} \right) \Delta X \Delta Y \Delta Z \tag{20.2-5}$$

Combining Eqs. 20.2-3 through 5 gives in the limit as $\Delta X \Delta Y \Delta Z$ goes to zero a continuity equation for Ψ_{iN}

$$\frac{\partial \Psi_{iN}}{\partial t} = -\left(\frac{\partial}{\partial \boldsymbol{Q}} \cdot [\dot{\boldsymbol{Q}} \Psi_{iN}] \right) + L_{iN}(Q, t) - \frac{\Psi_{iN}}{\lambda_{iN}(Q, t)} \tag{20.2-6}$$

This result differs from Eq. 13.2-12, obtained for dilute solutions of elastic dumbbells, in that creation and destruction terms are included. This latter distinction makes it more convenient to work in terms of Ψ_{iN} rather than the probability density ψ_N, which corresponds to ψ used in Chapter 13. Also the velocity space average $[\![\dot{\boldsymbol{Q}}]\!]$ in the elastic dumbbell theory is replaced by $\dot{\boldsymbol{Q}}$ in the network theory, since no account is taken of Brownian motion in the equation of motion for the segment vector.

c. The "Convection" Equation for $\Psi_{iN}(\boldsymbol{Q}, t)$

If we use Eq. 20.2-1 to replace $\dot{\boldsymbol{Q}}$ in Eq. 20.2-6 we obtain the *convection equation*

$$\boxed{\frac{\partial \Psi_{iN}}{\partial t} = -\left(\frac{\partial}{\partial \boldsymbol{Q}} \cdot [\boldsymbol{\kappa} \cdot \boldsymbol{Q}]\Psi_{iN}\right) + L_{iN}(Q, t) - \frac{\Psi_{iN}}{\lambda_{iN}(Q, t)}} \tag{20.2-7}$$

This is a first-order partial differential equation that describes how the segment distribution function Ψ_{iN} changes in time when the flow field is described by $\boldsymbol{\kappa}(t)$. Note that the corresponding "diffusion equation" in Eq. 13.2-13 is of second order.

By multiplying Eq. 20.2-7 by any function B of the segment vector $\boldsymbol{Q}$ and then integrating over all configuration space, we obtain an *equation of change* for $\langle B \rangle_{iN}$:

$$\frac{d}{dt}\langle B \rangle_{iN} = \boldsymbol{\kappa} : \left\langle \boldsymbol{Q}\frac{\partial B}{\partial \boldsymbol{Q}} \right\rangle_{iN} + \int L_{iN} B \, d\boldsymbol{Q} - \left\langle \frac{B}{\lambda_{iN}} \right\rangle_{iN} \tag{20.2-8}$$

where $\langle B \rangle_{iN} = \int B\Psi_{iN}\, d\boldsymbol{Q} = n_{iN} \int B\psi_N \, d\boldsymbol{Q}$ (*caution*: $\langle B \rangle_{iN}$ differs by a factor n_{iN} from the $\langle B \rangle$ defined in §12.4 and Eq. 13.1-5). The details of the integration follow closely those given in Example 13.2-1. If we generalize to the particular choice where $\mathbf{B}$ is a second-order tensor $\boldsymbol{QQ}$ then we find (see Example 20.2-1):

$$\langle \boldsymbol{QQ} \rangle_{iN(1)} = \bar{L}_{iN}(t)\boldsymbol{\delta} - \left\langle \frac{\boldsymbol{QQ}}{\lambda_{iN}} \right\rangle_{iN} \tag{20.2-9}$$

$$\bar{L}_{iN}(t) = \frac{4\pi}{3}\int_0^\infty L_{iN}(Q, t)Q^4 \, dQ \tag{20.2-10}$$

The derivation of Eq. 20.2-9 is given in Example 20.2-1 where this result is specialized to systems in which the probability of destruction λ_{iN} depends on time but not on the segment length Q. In Eq. 20.2-9 the subscript $_{(1)}$ notation denotes the convected time derivative defined in Eq. D.2-4a (note that the flow is homogeneous, so that the $\{\boldsymbol{v} \cdot \nabla \langle \boldsymbol{QQ} \rangle_{iN}\}$ contribution to the convected derivative is zero). We note that at equilibrium the creation and loss terms balance one another so that

$$\bar{L}_{iN,\,\mathrm{eq}}\boldsymbol{\delta} = \left\langle \frac{\boldsymbol{QQ}}{\lambda_{iN}} \right\rangle_{iN,\,\mathrm{eq}} \tag{20.2-11}$$

This result is used later to evaluate the pressure contribution from iN-segments.

EXAMPLE 20.2-1 Time Rate of Change of $\langle \boldsymbol{QQ} \rangle_{iN}$

Derive Eq. 20.2-9 by beginning with Eq. 20.2-8 written for the tensor $\mathbf{B} = \boldsymbol{QQ}$. Specialize this result for a network model in which the segment destruction probability is independent of Q, that is, $\lambda_{iN} = \lambda_{iN}(t)$.

SOLUTION For $\mathbf{B} = \boldsymbol{QQ}$ the equation of change Eq. 20.2-8 is rewritten

$$\frac{d}{dt}\langle \boldsymbol{QQ}\rangle_{iN} = \left\{\boldsymbol{\kappa}:\left\langle \boldsymbol{Q}\frac{\partial}{\partial \boldsymbol{Q}}\boldsymbol{QQ}\right\rangle_{iN}\right\} + \int L_{iN}(Q,t)\boldsymbol{QQ}\,d\boldsymbol{Q} - \left\langle \frac{\boldsymbol{QQ}}{\bar{\lambda}_{iN}(Q,t)}\right\rangle_{iN}$$

$$= \{\boldsymbol{\kappa}\cdot\langle \boldsymbol{QQ}\rangle_{iN} + \langle \boldsymbol{QQ}\rangle_{iN}\cdot\boldsymbol{\kappa}^{\dagger}\} + \int L_{iN}(Q,t)Q^4\,dQ\int \boldsymbol{uu}\,d\boldsymbol{u} - \left\langle \frac{\boldsymbol{QQ}}{\bar{\lambda}_{iN}}\right\rangle_{iN} \tag{20.2-12}$$

where we have rewritten the integral involving the creation term in spherical coordinates (Q, θ, ϕ). The vector $\boldsymbol{u} = \boldsymbol{Q}/Q$ is a unit vector in the direction of $\boldsymbol{Q}$, and $d\boldsymbol{u}$ denotes $\sin\theta\,d\theta\,d\phi$, where θ and ϕ are the spherical polar angles describing the orientation of $\boldsymbol{Q}$. The integral over $\boldsymbol{u}$ is easily done (cf. Eq. E.7-4)

$$\int \boldsymbol{uu}\,d\boldsymbol{u} = \frac{4\pi}{3}\boldsymbol{\delta} \tag{20.2-13}$$

and when this is combined with the definition for $\bar{L}_{iN}$ in Eq. 20.2-10, Eq. 20.2-9 is obtained.

We now consider the simplification in Eq. 20.2-9 that results when the segment loss rate is independent of Q. In this limit λ_{iN} can be taken outside of the configuration space average to give the following differential equation for $\langle \boldsymbol{QQ}\rangle_{iN}$:

$$\langle \boldsymbol{QQ}\rangle_{iN(1)} + \frac{1}{\bar{\lambda}_{iN}(t)}\langle \boldsymbol{QQ}\rangle_{iN} = \bar{L}_{iN}(t)\boldsymbol{\delta} \tag{20.2-14}$$

By using the methods of Chapter 9 (cf. Example 9.4-1) it is straightforward to integrate this result to get an explicit formula for $\langle \boldsymbol{QQ}\rangle_{iN}$. To do this we follow Example 9.4-1 and note that Eq. 20.2-14 can be rewritten as

$$\boldsymbol{\alpha}_{[1]}(t,t') + \frac{1}{\bar{\lambda}_{iN}(t')}\boldsymbol{\alpha}_{[0]}(t,t') = -\bar{L}_{iN}(t')\mathbf{B}(t,t') \tag{20.2-15}$$

where each term is understood to be evaluated at $t' = t$. Here we have abbreviated $\langle \boldsymbol{QQ}\rangle_{iN}$ by $\boldsymbol{\alpha}$, and we have replaced the unit tensor by[1]

$$\boldsymbol{\delta} = \mathbf{E}\cdot\mathbf{E}^{\dagger}|_{t'=t} = \mathbf{B}(t,t')|_{t'=t} \tag{20.2-16}$$

in which $\mathbf{E}$ is the deformation gradient (Eq. D.1-6) and $\mathbf{B}$ is the Finger strain tensor (Eq. D.3-4). We next replace $\boldsymbol{\alpha}_{[1]}$ by $\partial\boldsymbol{\alpha}_{[0]}/\partial t'$, and this gives a first order differential equation for $\boldsymbol{\alpha}_{[0]}$ that can be solved to give

$$\langle \boldsymbol{QQ}\rangle_{iN} = \int_{-\infty}^{t}\bar{L}_{iN}(t')\exp\left(\int_{t}^{t'}\bar{\lambda}_{iN}^{-1}(t'')dt''\right)\mathbf{B}(t,t')dt' \tag{20.2-17}$$

Notice that the average value $\langle \boldsymbol{QQ}\rangle_{iN}$ depends on the history of the deformation weighted by the creation and loss rates for the segments.

[1] The unit tensor could also be written as $\mathbf{B}^{-1}(t,t)$. That this is not the proper substitution is best seen by writing Eq. 20.2-14 in a convected coordinate system by using the outermost columns of Tables 9.3-1 and 9.4-1. In making this transformation, $\boldsymbol{\alpha}$ is treated like $\boldsymbol{\tau}$ in Table 9.4-1. Since the $_{(1)}$ notation denotes the convected derivative of the contravariant components of the tensor $\boldsymbol{\alpha}$, the inverse of the convected metric $\hat{g}^{ij}$ must be introduced on the right side of the equation during the coordinate transformation. Following the integration with respect to t', transformation back to the space fixed coordinate system transforms $\hat{g}^{ij}(t')$ to $\mathbf{B}(t,t')$.

EXAMPLE 20.2-2 The Distribution Function for a Network Solid

Determine the distribution function $\psi_N(\boldsymbol{Q}, t)$ for a solid polymer in which the network junctions are permanent chemical bonds. Use this distribution function to determine $\langle \boldsymbol{QQ} \rangle_N$. Note that for solids the subscript i, designating the segment complexity, is dropped. Since all segments are permanent, there is only one type of complexity.

SOLUTION For a solid, the convection equation, Eq. 20.2-7 simplifies considerably since segments are not destroyed, so that $\lambda_N \to \infty$; also all junctions are presumed to have been simultaneously created at time t_0. In keeping with assumption **(viii)** we take the distribution function for the network segments at the instant of creation to be the same as that of a set of freely jointed bead-rod chains with no constraints on the end points (that is, Gaussian). Thus from Eq. 11.3-21

$$L_N(t) = n_N \psi_{N,\text{eq}}(\boldsymbol{Q}_0)\delta(t - t_0) \tag{20.2-18}$$

where

$$\psi_{N,\text{eq}}(\boldsymbol{Q}_0) = \left(\frac{H_N}{2\pi kT}\right)^{3/2} e^{-(H_N/2kT)(\boldsymbol{Q}_0 \cdot \boldsymbol{Q}_0)} \tag{20.2-19}$$

Then the convection equation is

$$\frac{\partial \psi_N}{\partial t} = -\left(\frac{\partial}{\partial \boldsymbol{Q}} \cdot [\boldsymbol{\kappa} \cdot \boldsymbol{Q}]\psi_N\right) + \psi_{N,\text{eq}}(\boldsymbol{Q}_0)\delta(t - t_0) \tag{20.2-20}$$

where we have divided by the constant number density n_N.

The solution to Eq. 20.2-20 for $t > t_0$ may be obtained by inspection by noting that

$$\psi_{N,\text{eq}}(\boldsymbol{Q}_0)d\boldsymbol{Q}_0 = \psi_N(\boldsymbol{Q}, t)d\boldsymbol{Q} \qquad (t > t_0) \tag{20.2-21}$$

since the distortion of the segment vectors is equivalent to a change of variables in the distribution function. Thus the distribution function is (cf. Eq. 12.3-4b)

$$\begin{aligned}\psi_N(\boldsymbol{Q}, t) &= \psi_{N,\text{eq}}(\boldsymbol{Q}_0)\left|\frac{\partial}{\partial \boldsymbol{Q}}\boldsymbol{Q}_0\right| \\ &= \psi_{N,\text{eq}}(\boldsymbol{Q}_0)\det \boldsymbol{\Delta}(t, t_0) \\ &= \left(\frac{H_N}{2\pi kT}\right)^{3/2} e^{-(H_N/2kT)(\mathbf{B}^{-1}:\boldsymbol{QQ})} \qquad (t > t_0)\end{aligned} \tag{20.2-22}$$

where $\boldsymbol{\Delta} = \mathbf{E}^{-1}$ arises in the Jacobian of the transformation because of Eq. 20.2-2 (with $t' = t_0$). Since the deformation is at constant volume $\det \boldsymbol{\Delta} = 1$. Also in replacing $\boldsymbol{Q}_0$ by $\boldsymbol{Q}$ we introduce the Cauchy strain tensor $\mathbf{B}^{-1} = \{\boldsymbol{\Delta}^\dagger \cdot \boldsymbol{\Delta}\}$. If we now consider $t \le t_0$ as well as $t > t_0$, the δ-function in Eq. 20.2-18 causes a Heaviside unit step H function to be introduced into ψ_N:

$$\psi_N(\boldsymbol{Q}, t) = \left(\frac{H_N}{2\pi kT}\right)^{3/2} e^{-(H_N/2kT)(\mathbf{B}^{-1}:\boldsymbol{QQ})} H(t - t_0) \tag{20.2-23}$$

That Eq. 20.2-23 satisfies the convection equation Eq. 20.2-20 is easy to verify by direct substitution (see Problem 20B.4).

We next use the distribution function Eq. 20.2-22 to calculate $\langle \boldsymbol{QQ} \rangle_N$ for $t > t_0$. This is given by

$$\begin{aligned}
\langle \boldsymbol{QQ} \rangle_N &= \int \boldsymbol{QQ}\, \Psi_N(\boldsymbol{Q}, t) d\boldsymbol{Q} \\
&= n_N \int \boldsymbol{QQ}\, \psi_N(\boldsymbol{Q}, t) d\boldsymbol{Q} \\
&= n_N \int [\mathbf{E} \cdot \boldsymbol{Q}_0][\mathbf{E} \cdot \boldsymbol{Q}_0] \psi_{N,\mathrm{eq}}(\boldsymbol{Q}_0) d\boldsymbol{Q}_0 \\
&= n_N \{\mathbf{E} \cdot \int \boldsymbol{Q}_0 \boldsymbol{Q}_0 \left(\frac{H_N}{2\pi kT}\right)^{3/2} \exp(-(H_N/2kT)(\boldsymbol{Q}_0 \cdot \boldsymbol{Q}_0)) d\boldsymbol{Q}_0 \cdot \mathbf{E}^{\dagger}\} \\
&= n_N(\tfrac{1}{3}(N-1)a^2)\mathbf{B}(t, t_0) \qquad (t \geq t_0) \qquad (20.2\text{-}24)
\end{aligned}$$

Note that in computing this average it is simpler to change the integration variable to the undeformed state $\boldsymbol{Q}_0$, where the distribution function is that for equilibrium. This result could also be obtained by combining Eqs. 20.2-18 and 19 for $L_N(t)$ with Eq. 20.2-17 (with $\lambda_N^{-1} = 0$).

§20.3 THE EXPRESSION FOR THE STRESS TENSOR

According to the assumptions given in §20.1, the stress is produced solely by the network structure. In this section we use a simple physical argument similar to that given in §13.3 to deduce the expression for the stress tensor.

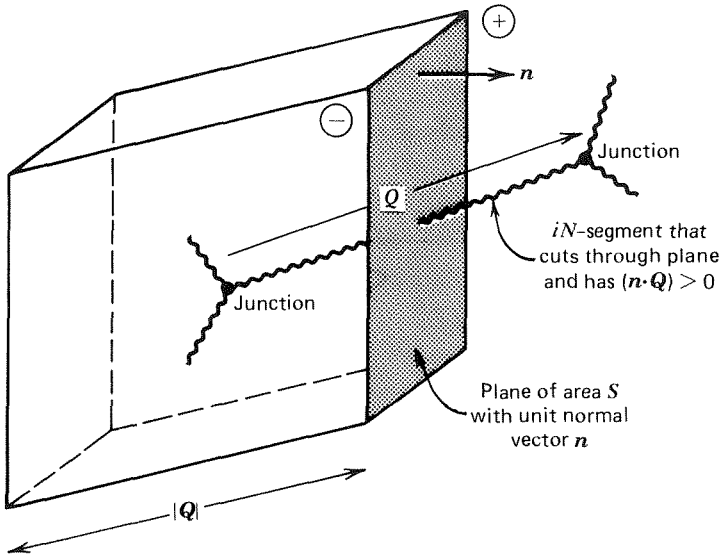

FIGURE 20.3-1. Physical argument used in calculating the contribution $\boldsymbol{\pi}_{iN}$ of segments of type iN to the stress tensor. The force per unit area exerted by − material ("behind" $\boldsymbol{n}$) on + material ("in front" of $\boldsymbol{n}$) is denoted by $[\boldsymbol{n} \cdot \boldsymbol{\pi}_{iN}]$. The tension in the strand $\boldsymbol{F}_N^{(c)} = F_N^{(c)}\, \boldsymbol{Q}/Q$ depends on the number of equivalent random links $(N-1)$ in the chain.

Consider an arbitrary plane of area S moving with the local material velocity that divides the material into two regions (Fig. 20.3-1). The only mechanism for the material on one side of this plane to transmit a force to the material on the other side is through the tension in the network segments that pass through the plane. To calculate this force we first note that the number of iN-network strands in the configuration range $\boldsymbol{Q}$ to $\boldsymbol{Q} + d\boldsymbol{Q}$ that intersect the plane is given by

$$|\boldsymbol{n} \cdot \boldsymbol{Q}| S \Psi_{iN}(\boldsymbol{Q}, t) d\boldsymbol{Q} \tag{20.3-1}$$

where $\boldsymbol{n}$ is the unit normal vector giving the orientation of the plane. The tension in the strand is $\boldsymbol{F}_N^{(c)} = F_N^{(c)} \boldsymbol{Q}/Q$ so that the force exerted by the material on the negative side of the plane on the positive side is

$$-\boldsymbol{F}_N^{(c)}, \quad \text{for} \quad (\boldsymbol{n} \cdot \boldsymbol{Q}) \geq 0; \qquad \boldsymbol{F}_N^{(c)}, \quad \text{for} \quad (\boldsymbol{n} \cdot \boldsymbol{Q}) < 0 \tag{20.3-2}$$

To get the total force per unit area of $-$ material on $+$ material due to iN-segments we take the product of the number of strands and the force from each strand divided by the area S and integrate over all configurations:

$$\begin{aligned}
[\boldsymbol{n} \cdot \boldsymbol{\pi}_{iN}] &= \int_{(\boldsymbol{n} \cdot \boldsymbol{Q}) > 0} (\boldsymbol{n} \cdot \boldsymbol{Q})(-\boldsymbol{F}_N^{(c)}) \Psi_{iN}(\boldsymbol{Q}, t) d\boldsymbol{Q} \\
&\quad + \int_{(\boldsymbol{n} \cdot \boldsymbol{Q}) < 0} (-\boldsymbol{n} \cdot \boldsymbol{Q})(\boldsymbol{F}_N^{(c)}) \Psi_{iN}(\boldsymbol{Q}, t) d\boldsymbol{Q} \\
&= -[\boldsymbol{n} \cdot \int \boldsymbol{Q} \boldsymbol{F}_N^{(c)} \Psi_{iN}(\boldsymbol{Q}, t) d\boldsymbol{Q}] \\
&= -[\boldsymbol{n} \cdot \langle \boldsymbol{Q} \boldsymbol{F}_N^{(c)} \rangle_{iN}]
\end{aligned} \tag{20.3-3}$$

Therefore the contribution to the total stress tensor from iN-segments is identified as

$$\begin{aligned}
\boldsymbol{\pi}_{iN} &= -\langle \boldsymbol{Q} \boldsymbol{F}_N^{(c)} \rangle_{iN} \\
&= -H_N \langle \boldsymbol{Q} \boldsymbol{Q} \rangle_{iN}
\end{aligned} \tag{20.3-4}$$

and the total stress tensor is

$$\boxed{\boldsymbol{\pi} = \sum_i \sum_N \boldsymbol{\pi}_{iN} = -\sum_i \sum_N H_N \langle \boldsymbol{Q} \boldsymbol{Q} \rangle_{iN}} \tag{20.3-5}$$

This expression for the total stress tensor is very similar to the intramolecular force contribution to the total stress tensor for elastic dumbbells (Eq. 13.3-5) and bead-spring chain models (Eq. 15.2-1).

To get the extra stress we write the total stress tensor as the sum of two parts:

$$\boldsymbol{\pi}_{iN} = p_{iN} \boldsymbol{\delta} + \boldsymbol{\tau}_{iN} \tag{20.3-6}$$

By definition $\boldsymbol{\tau}_{iN}$ is zero at equilibrium so that pressure p_{iN} is given by

$$p_{iN} \boldsymbol{\delta} = -\langle \boldsymbol{Q} \boldsymbol{F}^{(c)}(\boldsymbol{Q}) \rangle_{iN, \text{eq}} = -H_N \langle \boldsymbol{Q} \boldsymbol{Q} \rangle_{iN, \text{eq}} \tag{20.3-7}$$

where we have used the Gaussian assumption in replacing $\boldsymbol{F}_N^{(c)}$ in the last equality above.

EXAMPLE 20.3-1 Constitutive Equation for a Macromolecular Solid

(a) Show how Eqs. 20.3-4 and 5 can be specialized for a crosslinked polymeric solid. (b) Use this constitutive equation to calculate the stress-strain behavior in simple shear, pure shear, and elongation (Fig. 20.3-2).

SOLUTION (a) As in Example 20.2-2 we drop the subscript i on the stress tensor equation for a crosslinked solid with permanent junctions. The contribution to the stress tensor by an N-chain is easily evaluated with the aid of Eq. 20.2-24 in Example 20.2-2:

$$\boldsymbol{\pi}_N = -H_N\langle \boldsymbol{QQ}\rangle_N = -\tfrac{1}{3}n_N H_N(N-1)a^2\mathbf{B}(t,t_0) = -n_N kT\mathbf{B}(t,t_0) \tag{20.3-8}$$

In the last step, Eq. 11.3-20 has been used. The total stress tensor is then of the form

$$\boldsymbol{\pi} = -G_0\mathbf{B} \tag{20.3-9}$$

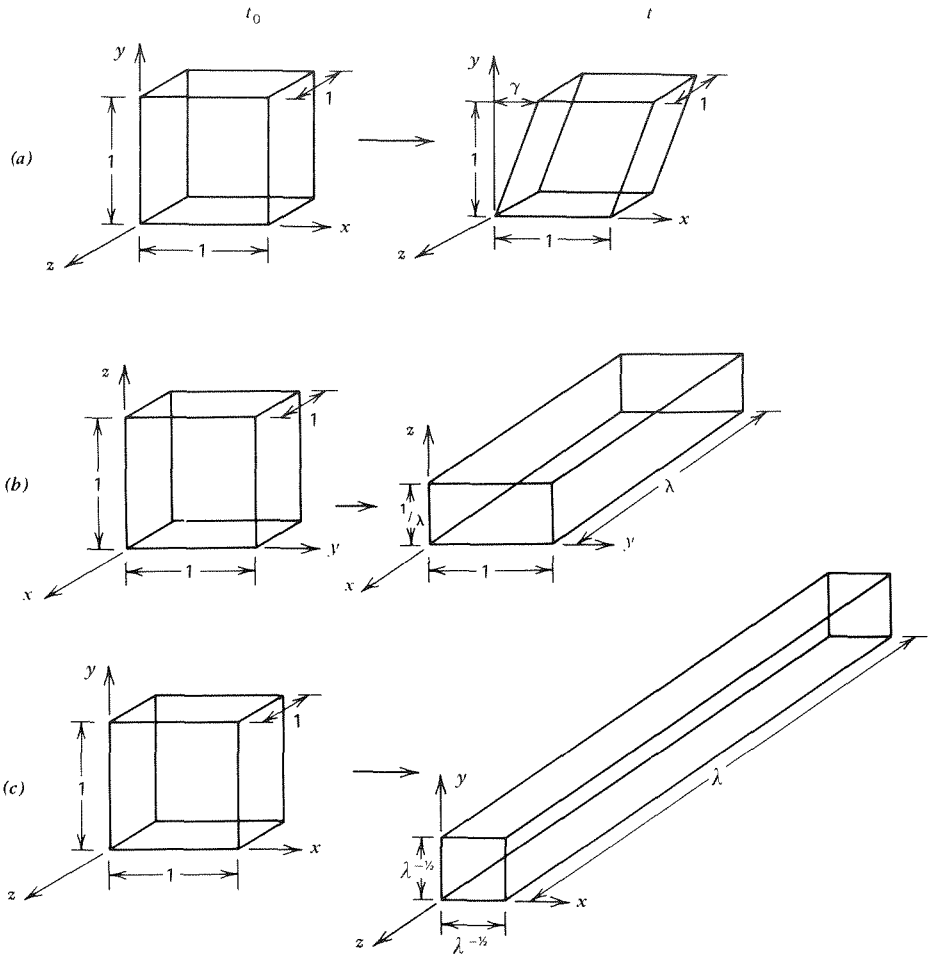

FIGURE 20.3-2. Deformations of a unit cube in (*a*) simple shear, (*b*) pure shear, and (*c*) elongation. The undeformed states t_0 are shown on the left and the deformed states t on the right. The orientation of the Cartesian axes in each part corresponds to the usage in part (*b*) of Example 20.3-2.

where the modulus G_0 is

$$\boxed{G_0 = \sum_N n_N kT = n_0 kT} \tag{20.3-10}$$

n_0 being the total number density of segments.

To get the extra stress τ we note that the pressure is from Eq. 20.3-7

$$p = -G_0 \tag{20.3-11}$$

and we obtain the constitutive equation for the elementary network model of a polymeric solid

$$\boxed{\tau = G_0 \gamma_{[0]}(t, t_0)} \tag{20.3-12}$$

For later comparison with the constitutive equations for network fluids, we note that Eq. 20.3-12 can be written in the equivalent differential form

$$\tau_{(1)}(t) = -G_0 \gamma_{(1)}(t) \tag{20.3-13}$$

This result is easily obtained with the aid of Problem 9B.5.

The modulus G_0 is often expressed in terms of the number density of junctions $n_0^\times$ rather than in terms of the number density of segments n_0. It is generally assumed that n_0 will be a small multiple s, say, of $n_0^\times$ such that

$$G_0 = s n_0^\times kT \tag{20.3-14}$$

The factor s will depend on the nature of the crosslinks introduced. For a network in which four segments meet at each junction, the factor s will be 2. In any event, s will seldom differ by very much from 2.

The constitutive equation Eq. 20.3-12 is often referred to as the equation of a "neo-Hookean" material. It is indeed quite remarkable that we have been able to obtain so easily a complete constitutive equation for the network model in a closed form. This equation provided the basis for the early work of Rivlin[1] on finite deformations of solids, and extensive[2] investigations have shown that the predictions are in excellent agreement with experimental results for moderate deformations.

Although the neo-Hookean solid is in good agreement with experimental observations at moderate deformations, it does not provide a complete description of the stress-strain relations for macromolecular solids. However, continuum mechanical arguments have been used to formulate a complete theory for large elastic deformations of solids. This development is primarily due to the theoretical and experimental works of Rivlin.[3]

(b) In order to be slightly more general in illustrating the material properties of network solids, we use in this part a generalization of the constitutive equation, Eq. 20.3-12, proposed originally by Mooney:[4]

$$\tau = G_0[(1 - q)\gamma_{[0]}(t, t_0) + q\gamma^{[0]}(t, t_0)] \tag{20.3-15}$$

[1] R. S. Rivlin, *Phil. Trans. Roy. Soc.* (London) **A240**, 459-490 (1948); **A240**, 491-508 (1948); **A240**, 509-525 (1948).

[2] The reader wishing a more comprehensive treatment with detailed comparisons with experiments is referred to L. R. G. Treloar, *The Physics of Rubber Elasticity*, 3rd. ed., Oxford University Press, London (1975). This book is attractively arranged to give a clear overview of the kinetic theory of rubber in the first five chapters. A useful review can be found in L. R. G. Treloar, *Rep. Progr. Phys.*, **36**, 755-826 (1973).

[3] A summary of this development is given by R. S. Rivlin, in F. R. Eirich, ed., *Rheology*, Vol. 1, Academic Press, New York (1956), pp. 351-385.

[4] M. Mooney, *J. Appl. Phys.*, **11**, 582-592 (1940).

Solids that follow Eq. 20.3-15 are called "Mooney" materials. When $q = 0$, the stress tensor depends linearly on the $\gamma_{[0]}$ tensor, and the Mooney equation reduces to the neo-Hookean equation. When $q = 1$, the stress tensor depends linearly on $\gamma^{[0]}$ defined in Eq. D.3-3. The inclusion of the $\gamma^{[0]}$ term in the equation, with q approximately equal to 0.1, gives improved agreement with experimental observations; however, the molecular origin of the $\gamma^{[0]}$ term is not clear.

(i) *Simple Shear*: Let the coordinates of a typical particle be x_0, y_0, z_0 in the undeformed state t_0 and x, y, z in the deformed state t. The displacement functions (Eq. D.1-4) relating the two sets of coordinates for simple shear are

$$\begin{cases} x = x_0 + \gamma y_0 \\ y = y_0 \\ z = z_0 \end{cases} \tag{20.3-16}$$

$$\begin{cases} x_0 = x - \gamma y \\ y_0 = y \\ z_0 = z \end{cases} \tag{20.3-17}$$

where γ is the "magnitude of shear" which is equal to the negative of the shear strain from state t to t_0 defined in Table C.1 as $\gamma_{yx}(t, t_0) = \int_t^{t_0} \dot{\gamma}_{yx}(t'')dt''$. From Table C.1 we see the deformation tensors are

$$\gamma_{[0]} = -\begin{pmatrix} \gamma^2 & \gamma & 0 \\ \gamma & 0 & 0 \\ 0 & 0 & 0 \end{pmatrix} \tag{20.3-18}$$

$$\gamma^{[0]} = -\begin{pmatrix} 0 & \gamma & 0 \\ \gamma & -\gamma^2 & 0 \\ 0 & 0 & 0 \end{pmatrix} \tag{20.3-19}$$

When these expressions are inserted into Eq. 20.3-15, we find the following nonzero stress components

$$\begin{aligned} \tau_{yx} &= \tau_{xy} = -G_0\gamma \\ \tau_{xx} - \tau_{yy} &= -G_0\gamma^2 \\ \tau_{yy} - \tau_{zz} &= qG_0\gamma^2 \end{aligned} \tag{20.3-20}$$

Note that the shear modulus is G_0, which is independent of q and of the magnitude of shear. In addition, we see that this macromolecular solid exhibits normal stress differences in shear, just as many macromolecular fluids exhibit normal stress differences in shear flow.

(ii) *Pure Shear*: The displacement functions are in pure shear (cf. Table C.1 with $b = 1$, and $\lambda_x = \lambda, \lambda_y = 1, \lambda_z = \lambda^{-1}$)

$$\begin{cases} x = \lambda x_0 \\ y = y_0 \\ z = \lambda^{-1} z_0 \end{cases} \tag{20.3-21}$$

$$\begin{cases} x_0 = \lambda^{-1} x \\ y_0 = y \\ z_0 = \lambda z \end{cases} \tag{20.3-22}$$

This deformation is obtained if a thin sheet of material oriented normal to the z-axis is clamped along two planes of constant x and then stretched by a factor of λ in the x-direction (Fig. 20.3-2b). From Table C.1 the deformation tensors are

$$\gamma_{[0]} = \begin{pmatrix} 1-\lambda^2 & 0 & 0 \\ 0 & 0 & 0 \\ 0 & 0 & 1-\lambda^2 \end{pmatrix} \tag{20.3-23}$$

$$\gamma^{[0]} = \begin{pmatrix} \lambda^{-2}-1 & 0 & 0 \\ 0 & 0 & 0 \\ 0 & 0 & \lambda^2-1 \end{pmatrix} \tag{20.3-24}$$

We then find the following nonzero stress differences

$$\tau_{xx} - \tau_{yy} = G_0[(1-2q) - (1-q)\lambda^2 - q\lambda^{-2}] \tag{20.3-25}$$

$$\tau_{xx} - \tau_{zz} = G_0[\lambda^{-2} - \lambda^2] \tag{20.3-26}$$

Hence if we let the surfaces of constant z be at atmospheric pressure p_a, we find that we must apply a force per unit area (measured in the stretched state) in the x-direction $-\pi_{xx}$ given by

$$\pi_{xx} = (\tau_{xx} - \tau_{zz}) + p_a = G_0(\lambda^{-2} - \lambda^2) + p_a \tag{20.3-27}$$

Note that π_{xx} is independent of q.

(iii) *Elongation*: The displacement functions are in elongation (cf. Table C.1 with $b = 0$, and $\lambda_x = \lambda_y = \lambda^{-1/2}$, $\lambda_z = \lambda$)

$$\begin{cases} x = \lambda^{-1/2} x_0 \\ y = \lambda^{-1/2} y_0 \\ z = \lambda z_0 \end{cases} \tag{20.3-28}$$

$$\begin{cases} x_0 = \lambda^{1/2} x \\ y_0 = \lambda^{1/2} y \\ z_0 = \lambda^{-1} z \end{cases} \tag{20.3-29}$$

This deformation is obtained if a long slender rod oriented in the z-direction is stretched by a ratio λ in the z-direction. The deformation tensors are

$$\gamma_{[0]} = \begin{pmatrix} 1-\lambda^{-1} & 0 & 0 \\ 0 & 1-\lambda^{-1} & 0 \\ 0 & 0 & 1-\lambda^2 \end{pmatrix} \tag{20.3-30}$$

$$\gamma^{[0]} = \begin{pmatrix} \lambda-1 & 0 & 0 \\ 0 & \lambda-1 & 0 \\ 0 & 0 & \lambda^{-2}-1 \end{pmatrix} \tag{20.3-31}$$

We then find the following stress differences:

$$\tau_{zz} - \tau_{xx} = G_0[(1-q)\lambda + q](\lambda^{-2} - \lambda) \tag{20.3-32}$$

$$\tau_{xx} - \tau_{yy} = 0 \tag{20.3-33}$$

Hence if the rod of material is surrounded by atmospheric pressure, we must apply a force per unit area (measured in the stretched state) in the z-direction $-\pi_{zz}$ given by

$$\pi_{zz} = (\tau_{zz} - \tau_{xx}) + p_a = G_0[(1-q)\lambda + q](\lambda^{-2} - \lambda) + p_a \tag{20.3-34}$$

in order to hold the material in the stretched state.

§20.4 THE LODGE NETWORK MODEL[1]

The Lodge network model is a generalization to multiple time constants of the single exponential constitutive equation of Green and Tobolsky. It is obtained by adding to the list of assumptions given in §20.1 that

x. (Lodge network model) The creation rates are independent of time $L_{iN} = L_{iN}(Q)$; the loss rates λ_{iN} are constants.

With L_{iN} and λ_{iN} given as above, Eq. 20.2-14 gives for $\langle \boldsymbol{QQ} \rangle_{iN}$:

$$\langle \boldsymbol{QQ} \rangle_{iN} + \lambda_{iN} \langle \boldsymbol{QQ} \rangle_{iN(1)} = \bar{L}_{iN} \lambda_{iN} \boldsymbol{\delta} \tag{20.4-1}$$

where $\bar{L}_{iN}$ given by Eq. 20.2-10 is now constant. In view of Eqs. 20.3-4 and 5, the stress tensor is then

$$\boldsymbol{\pi} = \sum_N \sum_i \boldsymbol{\pi}_{iN} \tag{20.4-2}$$

$$\boldsymbol{\pi}_{iN} + \lambda_{iN} \boldsymbol{\pi}_{iN(1)} = -H_N \bar{L}_{iN} \lambda_{iN} \boldsymbol{\delta} \tag{20.4-3}$$

By paralleling the development leading to Eq. 20.2-17 we can integrate Eq. 20.4-3 to get an explicit expression for the stress tensor:

$$\boldsymbol{\pi} = -\int_{-\infty}^{t} M(t-t') \mathbf{B}(t, t') dt' \tag{20.4-4}$$

$$M(t-t') = \sum_N H_N \sum_i \bar{L}_{iN} e^{-(t-t')/\lambda_{iN}} \tag{20.4-5}$$

In Eqs. 20.4-3 and 5 the spring constant H_N is given by $3kT/(N-1)a^2$ because of the assumption of Gaussian chains.

[1] A. S. Lodge, *Trans. Faraday Soc.*, **52**, 120–130 (1956); *Elastic Liquids*, Academic Press, New York (1964), pp. 118–120; *Rheol. Acta*, **7**, 379–392 (1968). The pioneering paper on the development of a constitutive equation for arbitrary deformations of a network model for fluids is that of M. S. Green and A. V. Tobolsky, *J. Chem. Phys.*, **14**, 80–92 (1946); see particularly Appendix B of this reference.

In order to write the constitutive equations for the extra stress τ we must subtract off the pressure contribution. This is found by evaluating Eq. 20.4-3 at equilibrium

$$p_{iN} = -H_N \bar{L}_{iN} \lambda_{iN} \tag{20.4-6}$$

The quantity $\bar{L}_{iN}$ can be evaluated since by assumption (viii) we take the Q-dependence of the creation rate to be the same as that for the equilibrium distribution function for freely jointed bead-rod chains with no constraints on the end points (Eq. 20.2-19). Thus if we denote by $\hat{L}_{iN}$ the constant creation rate of all iN-segments independent of segment length, then $L_{iN}(Q)$ is equal to $\hat{L}_{iN}\psi_{N,\mathrm{eq}}(Q)$ and we have

$$\begin{aligned}
\bar{L}_{iN} &= \frac{4\pi}{3} \hat{L}_{iN} \int_0^\infty \psi_{N,\mathrm{eq}}(Q) Q^4 \, dQ \\
&= \frac{4\pi}{3} \hat{L}_{iN} \left(\frac{H_N}{2\pi kT} \right)^{3/2} \int_0^\infty Q^4 e^{-(H_N/2kT)Q^2} \, dQ \\
&= \frac{1}{3} \hat{L}_{iN} \int Q^2 \psi_{N,\mathrm{eq}} \, d\boldsymbol{Q} \\
&= \frac{1}{3} \hat{L}_{iN} (N-1) a^2
\end{aligned} \tag{20.4-7}$$

Therefore

$$p_{iN} = -\hat{L}_{iN} kT \lambda_{iN} \tag{20.4-8}$$

and

$$p = \sum_N \sum_i p_{iN} \tag{20.4-9}$$

The constitutive equation for the extra stress tensor is then

$$\boxed{\boldsymbol{\tau} = \sum_j \boldsymbol{\tau}_j, \qquad \boldsymbol{\tau}_j + \lambda_j \boldsymbol{\tau}_{j(1)} = -\eta_j \boldsymbol{\gamma}_{(1)}} \tag{20.4-10}$$

or

$$\boxed{\begin{aligned} \boldsymbol{\tau} &= \int_{-\infty}^{t} M(t-t') \boldsymbol{\gamma}_{[0]}(t, t') \, dt' \\ M(t-t') &= \sum_j \frac{\eta_j}{\lambda_j^2} e^{-(t-t')/\lambda_j} \end{aligned}} \tag{20.4-11}$$

Here we have introduced $\sum_j$ to denote $\sum_N \sum_i$ and have rewritten the constant creation rate in terms of constants η_j with dimensions of viscosity

$$kT\hat{L}_j = \frac{\eta_j}{\lambda_j^2} \tag{20.4-12}$$

Equation 20.4-10 is identical to the generalized Maxwell model presented in Chapter 7 (Eqs. 7.6-1 and 7.6-2), and Eq. 20.4-11 was previously used in Chapter 8 (Eqs. 8.2-1 and 4).

The constants η_j (or $\hat{L}_j$) and λ_j are left undetermined by the theory. Note, however, that the relaxation modulus of linear viscoelasticity corresponding to $M(s)$ is

$$\boxed{G(s) = \sum_j \frac{\eta_j}{\lambda_j} e^{-s/\lambda_j}} \tag{20.4-13}$$

Hence the constants η_j and λ_j may be determined from the linear viscoelastic properties of a material (see Example 5.3-7).

It is clear that eventually the constants η_j (or $\hat{L}_j$) and λ_j, or appropriate replacements, should be obtained from detailed molecular calculations of the motions of the constituent macromolecules. In this way the dependence of the calculated material functions on molecular structure (for example, molecular weight, molecular weight distribution, and branching), which is presently missing in the network models, could be determined. Without developing such extensions of the theory, we can note a few features of the structure dependence. First, to the extent that the creation and loss of junctions are governed by thermal motions of the macromolecules (and it seems reasonable that this is the dominant mechanism at least for small deformations), $1/\lambda_j$ and $\hat{L}_j$ should depend on the equivalent number of random links (molecular weight) and temperature in the same way. One simple way to indicate this dependence is to let

$$\lambda_j \propto M^{\beta} a_T \tag{20.4-14}$$

$$\eta_j \propto M^{\beta} a_T \qquad (\hat{L}_j \propto M^{-\beta} a_T^{-1}) \tag{20.4-15}$$

where β is an unknown constant and a_T is a function of temperature. The function a_T is the "shift factor" in the method of time-temperature superposition (see §3.6 and Eqs. 15.3-31 through 33), and its inclusion in Eq. 20.4-14 is consistent with its normal use to scale time constants. The exponent β is expected to be positive, since the time required for overall macromolecular configuration changes increases with molecular weight.

It is interesting to note that the constitutive equation for the Lodge network model is very similar to the constitutive equations for chainlike bead-spring models of Rouse and Zimm for dilute solutions in Eqs. 15.3-17 and 15.4-21. The only difference is that the bead spring models give the relaxation modulus explicitly in terms of model parameters, whereas the network theory leaves the relaxation modulus undetermined. We can therefore easily adapt the material functions obtained for the Rouse–Zimm models (but not their molecular weight dependence).

In steady shear flow we find by analogy with Eqs. 15.3-25 through 27

$$\begin{aligned} \eta &= \eta_0 = \sum_j \eta_j \\ \Psi_1 &= \Psi_{10} = \sum_j 2\eta_j \lambda_j \\ \Psi_2 &= \Psi_{20} = 0 \end{aligned} \tag{20.4-16}$$

that is, the Lodge network model predicts shear-rate-independent viscometric functions, and the second normal stress coefficient is zero. Note that if Eqs. 20.4-14 and 15 are combined with Eqs. 20.4-16 we obtain

$$\begin{aligned} \eta_0 &\propto M^{\beta} \\ \Psi_{10} &\propto M^{2\beta} \end{aligned} \tag{20.4-17}$$

A value of β equal to 3.4 gives good agreement with structure property data on these material functions (cf. Figs. 3.6-4 and 7).

An exhaustive exploration of the predictions of the Lodge network model for a large number of homogeneous deformations has been given by Lodge.[2] In particular we call attention to the calculation[3] of the lateral expansion and longitudinal contraction exhibited by the Lodge network model if, at any instant in steady shear flow, all forces are suddenly removed from the fluid. Another interesting property of the Lodge network model is the prediction of stress relaxation upon cessation of steady shear flow that the shear stress should relax faster than the first normal stress difference, in agreement with experimental observations (§3.4, Experiment d). For elongational flow, the Lodge network model suffers from the same defect as the Rouse–Zimm models or the Hookean dumbbell: when the elongation rate equals $1/2\lambda_{\max}$, the elongational viscosity becomes infinite. Here $\lambda_{\max}$ is the largest of the λ_j. Moreover for $\dot{\varepsilon} > 1/2\lambda_{\max}$, start-up of steady elongational flow will never approach a steady state.

Finally we note that if it is desired to have information about molecular (segment) stretching and orientation, the distribution function Ψ_{iN} is available (Example 20.4-1). If it is desired to know how much the iN-segments are stretched by a flow, this can be obtained directly from Eq. 20.2-17:

$$\begin{aligned} \langle Q^2 \rangle_{iN} &= \tfrac{1}{3}(N-1)a^2\hat{L}_{iN}\int_{-\infty}^{t} e^{-(t-t')/\lambda_{iN}} \operatorname{tr} \mathbf{B}(t,t')dt' \\ &= (N-1)a^2\left[\hat{L}_{iN}\lambda_{iN} - \frac{1}{3kT}\operatorname{tr}\boldsymbol{\tau}_{iN}\right] \end{aligned} \tag{20.4-18}$$

The first line of Eq. 20.4-18 is more convenient if the deformation field is given. The second form is useful in suggesting ways to let the segment loss rates depend on the mean extension of segments through the trace of the stress tensor. We will investigate this latter possibility further in the next section.

EXAMPLE 20.4-1 The Segment Distribution Function for the Lodge Network Model

Find the segment distribution function Ψ_{iN} for the Lodge network model.

SOLUTION The convection equation for Ψ_{iN} for the Lodge network model is

$$\frac{\partial \Psi_{iN}}{\partial t} = -\frac{\partial}{\partial \boldsymbol{Q}}\cdot[\boldsymbol{\kappa}\cdot\boldsymbol{Q}]\Psi_{iN} + L_{iN}(Q) - \frac{\Psi_{iN}}{\lambda_{iN}} \tag{20.4-19}$$

[2] A. S. Lodge, *Elastic Liquids*, Academic Press, New York (1964), Chapters 6 and 7.

[3] A. S. Lodge, *Elastic Liquids*, Academic Press, New York (1964), pp. 131–139; see problem 20C.3.

where the λ_{iN} are constants. Since segments are assumed to be produced at a constant rate and with a distribution of configurations identical to an unconstrained bead-rod chain at equilibrium we have (cf. Eq. 20.2-18)

$$L_{iN}(Q) = \hat{L}_{iN}\psi_{N,\mathrm{eq}}(Q) = \hat{L}_{iN}\left(\frac{H_N}{2\pi kT}\right)^{3/2} e^{(H_N/2kT)(\mathbf{Q}\cdot\mathbf{Q})} \tag{20.4-20}$$

Note that, in contrast to Eq. 20.2-18, the above result involves only a single time t, at which the segments are created.

To solve Eq. 20.4-19, let us introduce two new terms

$$\dot{n}_{iN}(t, t')\,dt' = \text{number density of } iN\text{-segments created between time } t' \text{ and } t' + dt' \text{ that survive to time } t \tag{20.4-21}$$

$$\psi_N(\mathbf{Q}, t, t')\,d\mathbf{Q} = \text{fraction of segments with } (N-1) \text{ equivalent random links created at time } t' \text{ which are in the configuration range } \mathbf{Q} \text{ to } \mathbf{Q} + d\mathbf{Q} \text{ at time } t \tag{20.4-22}$$

In terms of these, Ψ_{iN} is

$$\Psi_{iN}(\mathbf{Q}, t) = \int_{-\infty}^{t} \dot{n}_{iN}(t, t')\psi_N(\mathbf{Q}, t, t')dt' \tag{20.4-23}$$

When Eq. 20.4-23 is put into Eq. 20.4-19 we see that

$$\hat{L}_{iN}\psi_{N,\mathrm{eq}}(Q) + \int_{-\infty}^{t} \frac{\partial}{\partial t}[\dot{n}_{iN}(t, t')\psi_N(\mathbf{Q}, t, t')]dt' = \int_{-\infty}^{t}\left[-\frac{\partial}{\partial \mathbf{Q}}\cdot[\boldsymbol{\kappa}\cdot\mathbf{Q}](\dot{n}_{iN}(t, t')\psi_N(\mathbf{Q}, t, t')) - \frac{\dot{n}_{iN}(t, t')\psi_N(\mathbf{Q}, t, t')}{\lambda_{iN}}\right]dt' + \hat{L}_{iN}\psi_{N,\mathrm{eq}}(Q) \tag{20.4-24}$$

where we have identified $\dot{n}_{iN}(t, t) = \hat{L}_{iN}$ as the constant creation rate of iN-segments.

Equation 20.4-24 can be satisfied provided that

$$\frac{\partial}{\partial t}\dot{n}_{iN}(t, t')\psi_N(\mathbf{Q}, t, t') = -\dot{n}_{iN}(t, t')\frac{\partial}{\partial \mathbf{Q}}\cdot[\boldsymbol{\kappa}\cdot\mathbf{Q}]\psi_N(\mathbf{Q}, t, t') - \frac{\dot{n}_{iN}(t, t')\psi_N(\mathbf{Q}, t, t')}{\lambda_{iN}} \tag{20.4-25}$$

It seems reasonable to postulate that (cf. Eq. 20.2-22)

$$\psi_N(\mathbf{Q}, t, t') = \left(\frac{H_N}{2\pi kT}\right)^{3/2} e^{-(H_N/2kT)(\mathbf{B}^{-1}(t,t'):\mathbf{QQ})} \tag{20.4-26}$$

whereupon in view of Eq. 20.2-20, $\dot{n}_{iN}(t, t')$ must satisfy

$$\frac{\partial}{\partial t}\dot{n}_{iN}(t, t') = -\frac{\dot{n}_{iN}(t, t')}{\lambda_{iN}} \tag{20.4-27}$$

subject to the initial condition

$$\dot{n}_{iN}(t', t') = \hat{L}_{iN} \tag{20.4-28}$$

The solution to Eqs. 20.4-27 and 28 is easily found:

$$\dot{n}_{iN}(t, t') = \hat{L}_{iN} e^{-(t-t')/\lambda_{iN}} \tag{20.4-29}$$

This means that the total number of iN-segments present at any time is

$$n_{iN}(t) = \int_{-\infty}^{t} \dot{n}_{iN}(t, t')dt' = \hat{L}_{iN}\lambda_{iN} \tag{20.4-30}$$

Finally, the segment distribution function is

$$\boxed{\Psi_{iN}(\underline{Q}, t) = \hat{L}_{iN}\left(\frac{H_N}{2\pi kT}\right)^{3/2} \int_{-\infty}^{t} e^{-(t-t')/\lambda_{iN}} e^{-(H_N/2kT)(\mathbf{B}^{-1}:\underline{Q}\underline{Q})}\, dt'} \tag{20.4-31}$$

Note that once Ψ_{iN} is available, it is possible to calculate the stress tensor directly from Eq. 20.3-4. This is easily done either by interchanging the order of the time and $\underline{Q}$-integrations and then performing the configuration average by using the steps shown in Eq. 20.2-24, or by using Eq. E.3-3.

§20.5 MODIFIED NETWORK MODELS FOR MACROMOLECULAR FLUIDS

Several modified network models have been proposed to improve on the rheological predictions of the Lodge rubberlike liquid. A first group of modifications has focused on using more realistic segment kinetics assumptions. Indeed the assumption used in the previous section that the segment creation and loss rates are entirely independent of the deformation history seems rather unlikely, particularly for the destruction term. It seems plausible that large deformations and stresses would influence the rates at which segments are created and lost. For example, the infinite elongational viscosity of the Lodge model is easily shown to correspond to the fact that the segments are stretched to infinite length, in the same way as Hookean dumbbells were found to stretch infinitely far in elongational flows (Eqs. 13.4-34 and 35). We intuitively feel that one or both of the end junctions for these segments should break and that the segments should be lost from the network, rather than be allowed to stretch this drastically. A second modification of the rubberlike liquid model relaxes the affine motion assumption.

Below we give a brief discussion of several network models that illustrate these two kinds of modifications of the rubberlike liquid model. The discussion is not exhaustive, but is rather intended to give the reader an introduction to the research activities in this area. We discuss the nonaffine motion first, since it is somewhat simpler to treat, and it can then be used together with any modifications to the segment kinetics.

a. Non-Affine Motion

Here we consider a modification, which was proposed by Phan-Thien and Tanner,[1] to assumption (iii) that the junctions move affinely. We continue to neglect the thermal motions of the junctions.

[1] N. Phan-Thien and R. I. Tanner, *J. Non-Newtonian Fluid Mech.*, **2**, 353–365 (1977); N. Phan-Thien, *J. Rheol.*, **22**, 259–283 (1978); R. I. Tanner, *J. Non-Newtonian Fluid Mech.*, **5**, 103–112 (1979).

Let us denote by $\boldsymbol{r}_\nu$ the position of an arbitrary junction ν. Phan-Thien and Tanner proposed that the motion of this junction be given by

$$\dot{\boldsymbol{r}}_\nu = \boldsymbol{v}_0 + [\boldsymbol{\kappa}\cdot\boldsymbol{r}_\nu] - \tilde{\boldsymbol{v}}(\boldsymbol{r}_\nu) \tag{20.5-1}$$

where $\tilde{\boldsymbol{v}}(\boldsymbol{r})$ is a "slip velocity" that accounts for the inability of the junctions to follow the macroscopically imposed velocity field exactly. Now let $\boldsymbol{r}_\mu$ be the position of a second junction connected to $\boldsymbol{r}_\nu$ by the segment with end-to-end vector $\boldsymbol{Q}$:

$$\boldsymbol{r}_\mu - \boldsymbol{r}_\nu = \boldsymbol{Q} \tag{20.5-2}$$

The velocity of $\boldsymbol{r}_\mu$ is also given by Eq. 20.5-1. Subtracting the equation for $\dot{\boldsymbol{r}}_\nu$ from that for $\dot{\boldsymbol{r}}_\mu$ gives

$$\begin{aligned}\dot{\boldsymbol{Q}} &= [\boldsymbol{\kappa}\cdot\boldsymbol{Q}] - [\tilde{\boldsymbol{v}}(\boldsymbol{r}_\mu) - \tilde{\boldsymbol{v}}(\boldsymbol{r}_\nu)] \\ &= [\boldsymbol{\kappa}\cdot\boldsymbol{Q}] - [\nabla\tilde{\boldsymbol{v}}^\dagger\cdot\boldsymbol{Q}] + \cdots \\ &\doteq [\hat{\boldsymbol{\kappa}}\cdot\boldsymbol{Q}]\end{aligned} \tag{20.5-3}$$

In going from the first to the second line of Eq. 20.5-3 we have expanded the slip velocity at junction $\boldsymbol{r}_\mu$ in a Taylor series about $\boldsymbol{r}_\nu$ and kept only the first two terms. This truncation should be a reasonable approximation if Q is small compared to the macroscopic length scale over which $\tilde{\boldsymbol{v}}$ varies. In the last line above we have introduced the "effective velocity gradient tensor" (cf. Problem 13B.2)

$$\begin{aligned}\hat{\boldsymbol{\kappa}} &= \boldsymbol{\kappa} - \nabla\tilde{\boldsymbol{v}}^\dagger \\ &= \boldsymbol{\kappa} - \tilde{\boldsymbol{\kappa}}\end{aligned} \tag{20.5-4}$$

of the effective macroscopic velocity field

$$\hat{\boldsymbol{v}} = \boldsymbol{v}_0 + [\boldsymbol{\kappa}\cdot\boldsymbol{r}] - \tilde{\boldsymbol{v}} \tag{20.5-5}$$

Finally, we assume that the "slip tensor" $\tilde{\boldsymbol{\kappa}}$ can be given by[2]

$$\tilde{\boldsymbol{\kappa}} = \tfrac{1}{2}\xi\dot{\boldsymbol{\gamma}} \tag{20.5-6}$$

in which ξ is an arbitrary "slip constant" and $\dot{\boldsymbol{\gamma}} = \boldsymbol{\kappa} + \boldsymbol{\kappa}^\dagger$ is the rate of strain tensor for the macroscopically imposed velocity field.

When Eqs 20.5-3 through 6 are combined we get the equation of motion for the segment vector

$$\dot{\boldsymbol{Q}} = [\boldsymbol{\kappa}\cdot\boldsymbol{Q}] - \tfrac{1}{2}\xi[\dot{\boldsymbol{\gamma}}\cdot\boldsymbol{Q}] \tag{20.5-7}$$

Equation 20.5-7 replaces Eq. 20.2-1 in the non-affine motion modification to the network theory. Note that slip is completely described by ξ.

[2] Phan-Thien and Tanner (*op.cit.*) assume a slightly different form for $\tilde{\boldsymbol{\kappa}}$ which leads to an additional term $-\sigma\boldsymbol{Q}$ on the right of Eq. 20.5-7. This term must be excluded, since for a fluid at rest ($\boldsymbol{v} = \boldsymbol{0}$), the modified Eq. 20.5-7 would give $Q \to 0$ or ∞ depending on whether $\sigma > 0$ or $\sigma < 0$. Both alternatives are physically unreasonable.

The entire development leading up to the constitutive equaiton for the Lodge network model can now be paralleled by simply replacing $\boldsymbol{v}$ everywhere by $\hat{\boldsymbol{v}}$ (and $\boldsymbol{\kappa}$ by $\hat{\boldsymbol{\kappa}}$). This leads to the following differential form of the extra stress tensor (cf. Eq. 20.4-10):

$$\boxed{\boldsymbol{\tau} = \sum_j \boldsymbol{\tau}_j} \tag{20.5-8}$$

$$\boldsymbol{\tau}_j + \lambda_j \left\{ \frac{\partial}{\partial t} \boldsymbol{\tau}_j - \hat{\boldsymbol{\kappa}} \cdot \boldsymbol{\tau}_j - \boldsymbol{\tau}_j \cdot \hat{\boldsymbol{\kappa}}^\dagger \right\} = -\eta_j (\hat{\boldsymbol{\kappa}} + \hat{\boldsymbol{\kappa}}^\dagger) \tag{20.5-9}$$

When $\hat{\boldsymbol{\kappa}}$ is rewritten in terms of $\boldsymbol{\kappa}$ and $\frac{1}{2}\xi\dot{\boldsymbol{\gamma}}$ we obtain

$$\boxed{\begin{aligned} &\boldsymbol{\tau}_j + \hat{\lambda}_j \boldsymbol{\tau}_{j(1)} + \tfrac{1}{2}\hat{\lambda}_j \xi \{\dot{\boldsymbol{\gamma}} \cdot \boldsymbol{\tau}_j + \boldsymbol{\tau}_j \cdot \dot{\boldsymbol{\gamma}}\} = -\hat{\eta}_j \dot{\boldsymbol{\gamma}} \\ &\text{or} \\ &\boldsymbol{\tau}_j + \hat{\lambda}_j \boldsymbol{\tau}_{j(\hat{1})} = -\hat{\eta}_j \dot{\boldsymbol{\gamma}} \end{aligned}} \tag{20.5-10}$$

where

$$\hat{\eta}_j = \eta_j (1 - \xi) \tag{20.5-11}$$

gives the relation between the creation rate constants η_j in the Lodge network model and the coefficients appearing naturally in Eq. 20.5-10. In the second form of Eq. 20.5-10, the notation $_{(\hat{1})}$ denotes the convected derivative calculated with the effective velocity gradient $\hat{\boldsymbol{\kappa}}$. The integral form of the constitutive equation with non-affine motion can also be written down immediately from Eq. 20.4-11:

$$\boxed{\begin{aligned} \boldsymbol{\tau} &= \int_{-\infty}^{t} M(t - t')(1 - \xi)^{-1} \hat{\boldsymbol{\gamma}}_{[0]}(t, t') dt' \\ M(t - t') &= \sum_j \frac{\hat{\eta}_j}{\lambda_j^2} e^{-(t - t')/\lambda_j} \end{aligned}} \tag{20.5-12}$$

The tensor $\hat{\boldsymbol{\gamma}}_{[0]}$ is a modified finite strain tensor which is computed from the velocity field $\hat{\boldsymbol{v}}$ rather than from $\boldsymbol{v}$. The factor of $(1 - \xi)^{-1}$ is included in Eq. 20.5-12, because $(1 - \xi)^{-1}\hat{\boldsymbol{\gamma}}_{[0]}$ simplifies to the infinitesimal strain tensor in the limit of small deformations. If linear viscoelastic data are used to determine the $\hat{\eta}_j$ and λ_j in Eqs. 20.5-10 or 12, then the resulting values will be numerically equal to the η_j and λ_j found for the Lodge network model.

The differential form of the constitutive equation[3] is a special case of the Oldroyd 8-constant model discussed in detail in §7.3 (cf. Eq. 7.3-2). As is shown in Example 20.5-1, the non-affine motion assumption leads to a shear-rate-dependent viscosity. However, the viscosity decreases too rapidly with shear rate, and the negative of the shear stress goes through a maximum with increasing shear rate, which is physically unreasonable. In addition, the elongational viscosity becomes infinite at finite elongation rates. Although these critical elongation rates are slightly different than those found for the Lodge network

[3] A similar model was developed from purely continuum arguments by M. W. Johnson, Jr. and D. Segalman, *J. Non-Newtonian Fluid Mech.*, **2**, 255-270 (1977).

model, the infinite value of $\bar{\eta}$ is unrealistic. Thus modification of only the affine motion assumption in the Lodge network model (at least in the way done here) does not lead to substantial improvements in the rheological predictions, so we turn in the next subsection to consideration of non-constant segment creation rates and loss probabilities.

EXAMPLE 20.5-1 Rheological Properties of a Non-Affine Lodge Network Model

Consider the constitutive equations obtained from relaxing the affine motion assumption in the Lodge network model (Eqs. 20.5-8, 10 and 12). Determine the (a) viscometric properties and (b) elongational viscosity for this model.

SOLUTION **(a)** Steady Shear Flow

For steady shear flow with shear rate $\dot{\gamma}$ we can use the entries in Table C.1 to write Eq. 20.5-10 in matrix form:

$$\begin{pmatrix} \tau_{jxx} & \tau_{jyx} & 0 \\ \tau_{jyx} & \tau_{jyy} & 0 \\ 0 & 0 & \tau_{jzz} \end{pmatrix} - \lambda_j\dot{\gamma}\begin{pmatrix} 2\tau_{jyx} & \tau_{jyy} & 0 \\ \tau_{jyy} & 0 & 0 \\ 0 & 0 & 0 \end{pmatrix}$$

$$+ \tfrac{1}{2}\xi\lambda_j\dot{\gamma}\begin{pmatrix} 2\tau_{jyx} & (\tau_{jxx}+\tau_{jyy}) & 0 \\ (\tau_{jxx}+\tau_{jyy}) & 2\tau_{jyx} & 0 \\ 0 & 0 & 0 \end{pmatrix} = -\hat{\eta}_j\dot{\gamma}\begin{pmatrix} 0 & 1 & 0 \\ 1 & 0 & 0 \\ 0 & 0 & 0 \end{pmatrix} \tag{20.5-13}$$

The equations for the stress components are then

$$\tau_{jxx} - 2\lambda_j\dot{\gamma}\,\tau_{jyx}(1 - \tfrac{1}{2}\xi) = 0 \tag{20.5-14}$$

$$\tau_{jyx} - \lambda_j\dot{\gamma}(\tau_{jyy} - \tfrac{1}{2}\xi(\tau_{jxx} + \tau_{jyy})) = -\hat{\eta}_j\dot{\gamma} \tag{20.5-15}$$

$$\tau_{jyy} + \lambda_j\xi\dot{\gamma}\,\tau_{jyx} = 0 \tag{20.5-16}$$

$$\tau_{jzz} = 0 \tag{20.5-17}$$

When these are solved we get the viscometric functions

$$\eta(\dot{\gamma}) = -\sum_j \frac{\tau_{jyx}}{\dot{\gamma}} = \sum_j \frac{\hat{\eta}_j}{[1 + \xi(2-\xi)(\lambda_j\dot{\gamma})^2]} \tag{20.5-18}$$

$$\Psi_1(\dot{\gamma}) = -\sum_j \frac{(\tau_{jxx} - \tau_{jyy})}{\dot{\gamma}^2} = \sum_j \frac{2\lambda_j\hat{\eta}_j}{[1 + \xi(2-\xi)(\lambda_j\dot{\gamma})^2]} \tag{20.5-19}$$

$$\Psi_2(\dot{\gamma}) = -\sum_j \frac{(\tau_{jyy} - \tau_{jzz})}{\dot{\gamma}^2} = -\frac{\xi}{2}\Psi_1 \tag{20.5-20}$$

At high shear rates it is seen that $\eta \propto \dot{\gamma}^{-2}$ which is physically impossible; however, this asymptotic behavior is not reached until $\dot{\gamma} \gg 1/\lambda_{\min}$ where $\lambda_{\min}$ is the smallest of the empirically fit time constants. The asymptotic behavior of Ψ_1 is also proportional to $\dot{\gamma}^{-2}$, which is much closer to experimental observations at high shear rates. From Eq. 20.5-20 we see that if Ψ_2 can be measured, then its ratio to Ψ_1 can be used to determine the slip parameter ξ. Experimental data on polymer melts and concentrated solutions suggests a value of ξ in the range $0.1 < \xi < 0.5$.

In the absence of experimental data on Ψ_2, ξ can be estimated from comparisons of $\eta(\dot{\gamma})$ and $\eta'(\omega)$. For small rates of deformation, Eqs. 20.5-8 and 10 reduce to the Lodge network model Eq. 20.4-10 (with η_j replaced by $\hat{\eta}_j$) which is the same as the Rouse model Eq. 15.3-17 (with $\eta_s = 0$ $\eta_j = nkT\lambda_j$ and the λ_j undetermined). The small amplitude oscillatory shearing properties are then given by Eqs. 15.3-29 and 30. For η' we have

$$\eta' = \sum_j \frac{\hat{\eta}_j}{[1 + (\lambda_j\omega)^2]} \tag{20.5-21}$$

Comparing η and η' shows

$$\eta(\dot{\gamma}) = \eta'(\omega)|_{\omega = \sqrt{\xi(2-\xi)}\dot{\gamma}} \tag{20.5-22}$$

Thus the viscosity curve is identical to the η' curve except that it is shifted to the right on the shear rate/frequency axis by a factor of $\sqrt{\xi(2-\xi)}$. This horizontal displacement is not actually observed experimentally. Although η does lie above η' at high frequencies and shear rates, the two curves have different slopes with η' decreasing more rapidly than η. Nonetheless, the difference in η and η' at large $\dot{\gamma}$ and ω can be approximated by a horizontal shift, and the magnitude of the shift gives ξ.

(b) Elongational Flow

For steady elongational flow with elongation rate $\dot{\varepsilon}$ we can again use Table C.1 to find the contributions to the constitutive equation Eq. 20.5-10. When these are combined we have

$$\begin{pmatrix} \tau_{jxx} & 0 & 0 \\ 0 & \tau_{jyy} & 0 \\ 0 & 0 & \tau_{jzz} \end{pmatrix} - \lambda_j\dot{\varepsilon}(1-\xi)\begin{pmatrix} -\tau_{jxx} & 0 & 0 \\ 0 & -\tau_{jyy} & 0 \\ 0 & 0 & 2\tau_{jzz} \end{pmatrix} = -\hat{\eta}_j\dot{\varepsilon}\begin{pmatrix} -1 & 0 & 0 \\ 0 & -1 & 0 \\ 0 & 0 & 2 \end{pmatrix} \tag{20.5-23}$$

The stress components are given by

$$\tau_{jxx} = \tau_{jyy} = \frac{\hat{\eta}_j\dot{\varepsilon}}{[1 + (1-\xi)\lambda_j\dot{\varepsilon}]} \tag{20.5-24}$$

$$\tau_{jzz} = \frac{-2\hat{\eta}_j\dot{\varepsilon}}{[1 - 2(1-\xi)\lambda_j\dot{\varepsilon}]} \tag{20.5-25}$$

Thus the elongational viscosity is given by

$$\bar{\eta} = -\frac{\tau_{zz} - \tau_{xx}}{\dot{\varepsilon}} = 3\sum_j \frac{\hat{\eta}_j}{[1 + (1-\xi)\lambda_j\dot{\varepsilon}][1 - 2(1-\xi)\lambda_j\dot{\varepsilon}]} \tag{20.5-26}$$

An infinite value of $\bar{\eta}$ is found when either

$$\dot{\varepsilon} = -\frac{1}{(1-\xi)\lambda_{\max}} \quad \text{or} \quad \dot{\varepsilon} = \frac{1}{2(1-\xi)\lambda_{\max}} \tag{20.5-27}$$

For values of ξ between 0.1 and 0.5, these critical strain rates are within a factor of two of the critical elongation rates found for Hookean dumbbells (cf. Eq. 13.4-36).

b. Time-Dependent Segment Creation and Loss Rates

Let us replace assumption (x) used in the Lodge network model by:

x′. The creation and loss rates can be functions of time.

With this additional generality most of the development leading up to the constitutive equation in §20.4 can be taken over with only slight modification. This leads to the following constitutive equation for the contribution of iN-segments to the total stress tensor

$$\boxed{\boldsymbol{\pi}_{iN} + \lambda_{iN}(t)\boldsymbol{\pi}_{iN(1)} = -kT\hat{L}_{iN}(t)\lambda_{iN}(t)\boldsymbol{\delta}} \tag{20.5-28}$$

which is equivalent to Eq. 20.4-3 with λ_{iN} and $\hat{L}_{iN}$ allowed to depend on time. Also in writing Eq. 20.5-28 we have assumed that segments are created with a Gaussian distribution so that $\bar{L}_{iN}$ can be replaced by the rate of creation of all iN-segments $\hat{L}_{iN}$ by means of Eq. 20.4-7. The pressure contribution, obtained by evaluating the above at equilibrium, is

$$p_{iN} = -kT\hat{L}_{iN,\,\mathrm{eq}}\lambda_{iN,\,\mathrm{eq}} = -n_{iN,\,\mathrm{eq}}kT \tag{20.5-29}$$

in which the subscript $_{\mathrm{eq}}$ denotes an equilibrium value. By subtracting $p_{iN}\boldsymbol{\delta}$ from $\boldsymbol{\pi}_{iN}$ we get a constitutive equation for the extra stress

$$\boxed{\boldsymbol{\tau}_{iN} + \lambda_{iN}(t)\boldsymbol{\tau}_{iN(1)} = -kT\hat{L}_{iN,\,\mathrm{eq}}\lambda_{iN,\,\mathrm{eq}}\lambda_{iN}(t)\dot{\boldsymbol{\gamma}} - kT[\hat{L}_{iN}(t)\lambda_{iN}(t) - \hat{L}_{iN,\,\mathrm{eq}}\lambda_{iN,\,\mathrm{eq}}]\boldsymbol{\delta}} \tag{20.5-30}$$

The integral forms of Eqs. 20.5-28 and 30 give the following constitutive equations for the total stress tensor and the extra stress tensor, respectively:

$$\boxed{\boldsymbol{\pi} = -\int_{-\infty}^{t} M(t, t')\mathbf{B}(t, t')dt'} \tag{20.5-31}$$

$$\boxed{\boldsymbol{\tau} = \sum_j n_{j,\,\mathrm{eq}}kT\boldsymbol{\delta} - \int_{-\infty}^{t} M(t, t')\mathbf{B}(t, t')dt'} \tag{20.5-32}$$

where

$$M(t, t') = kT\sum_j \hat{L}_j(t')\exp\left[-\int_{t'}^{t}\lambda_j^{-1}(t'')dt''\right] \tag{20.5-33}$$

where the sums on i and N have again been abbreviated as a single sum on j. Two differences between these results and Eqs. 20.4-4, 5 and 11 are evident. First, the memory function M now depends on t and t' separately, rather than only on their difference, $t - t'$. Second, the equation for the extra stress is now written more conveniently in terms of $\mathbf{B}$ than in terms of $\boldsymbol{\gamma}_{[0]}$, because of the time dependence of $\hat{L}_{iN}$ and λ_{iN}. If information is desired about the deformation of the segments during flow, this can be obtained from Eq. 20.2-17 with $\bar{L}_{iN}$ replaced by $\frac{1}{3}(N-1)a^2\hat{L}_{iN}$.

We now describe three models which can be obtained from the general constitutive equations above by making specific assumptions about the segment kinetics. These are the models of Acierno, La Mantia, Marrucci, and Titomanlio, of Wagner, and of Phan-Thien and Tanner.

The Acierno, La Mantia, Marrucci, and Titomanlio Model[4]

Although not originally developed as a molecular network theory, it has been shown by Jongschaap[5] that this model can be derived from a network theory in which the creation and loss rates are given by

$$\hat{L}_j(t) \equiv \int L_j(Q, t)dQ = \frac{n_j(t)}{\nu_j(t)} \tag{20.5-34}$$

$$\frac{1}{\lambda_j(t)} = \frac{1}{\nu_j(t)}\left(\alpha\sqrt{\frac{-\text{tr}\,\tau_j}{2G_j}} - \frac{1}{x_j} + 2\right) \tag{20.5-35}$$

in which $\nu_j(t)$ is a time "constant" for creation, α is an adjustable constant, and x_j is the number density of j-segments at time t divided by the equilibrium number density

$$x_j = \frac{n_j}{n_{j,\text{eq}}} \tag{20.5-36}$$

The G_j are moduli given by

$$G_j = n_j kT \tag{20.5-37}$$

The functions ν_j describing creation are assumed to depend on x_j as follows:

$$\nu_j(t) = \nu_{j,\text{eq}} x_j(t)^{1.4} \tag{20.5-38}$$

The exponent of 1.4 on x_j in this equation is chosen so that the zero-shear-rate viscosity is proportional to $n^{3.4}$ where n is the total number density of segments. Allowing the segment loss rates to depend on the trace of the extra stress tensor as is done in Eq. 20.5-35 would seem to be a reasonable postulate in view of the connection between segment stretching and $\text{tr}\,\tau_j$ (cf. Eq. 20.4-18).

To obtain the memory function for this model we begin by integrating the convection equation, Eq. 20.2-7, over all configurations Q. If we use the divergence theorem on the first term on the right side of Eq. 20.2-7 and assert that $\Psi_j \to 0$ as $Q \to \infty$ then we obtain[6]

$$\frac{\partial n_j}{\partial t} = \hat{L}_j - \frac{n_j}{\lambda_j} = n_j\left(\frac{1}{\nu_j} - \frac{1}{\lambda_j}\right) \tag{20.5-39}$$

[4] D. Acierno, F. P. La Mantia, G. Marrucci, and G. Titomanlio, *J. Non-Newtonian Fluid Mech.*, **1**, 125–146 (1976); see also H. Janeschitz-Kriegl, *Polymer Melt Rheology and Flow Birefringence*, Springer, Berlin (1983), §2.5.5. The differential form of the model as originally proposed is given as Eq. E in Table 7.6-1.

[5] R. J. J. Jongschaap, *J. Non-Newtonian Fluid Mech.*, **8**, 183–190 (1983).

[6] Equation 20.5-39 corresponds to Acierno et al.'s equation for the "structure" variable x_j. Their equation is obtained from Eq. 20.5-39 by replacing n_j by x_j (Eq. 20.5-36) and by using Eq. 20.5-35 for λ_j.

The solution for the number density of segments is

$$n_j(t) = n_j(t') \exp\left[\int_{t'}^{t}\left(\frac{1}{\nu_j(t'')} - \frac{1}{\lambda_j(t'')}\right)dt''\right]$$
$$= \hat{L}_j(t')\nu_j(t') \exp\left[\int_{t'}^{t}\left(\frac{1}{\nu_j(t'')} - \frac{1}{\lambda_j(t'')}\right)dt''\right] \tag{20.5-40}$$

where in the second line we have used Eq. 20.5-34 to write the number density at t' in terms of the creation rate. Finally we solve Eq. 20.5-40 for $\hat{L}_j$ and combine this result with Eq. 20.5-33 to get the memory function

$$M(t, t') = kT \sum_j \hat{L}_j(t') \exp\left[-\int_{t'}^{t}\frac{1}{\lambda_j(t'')}dt''\right]$$
$$= \frac{n_j(t)kT}{\nu_j(t')} \exp\left[-\int_{t'}^{t}\frac{1}{\nu_j(t'')}dt''\right] \tag{20.5-41}$$

When written as in the bottom line above, the relaxation times for the model are seen to be associated with segment creation rates rather than segment loss rates as found in the Lodge network model or the Wagner or Phan-Thien–Tanner models to be discussed next. Acierno, La Mantia, Marrucci, and Titomanlio[7] report that good fits to low density polyethylene data can be obtained with Eqs. 20.5-32 and 41.

Phan-Thien–Tanner Model

Another model in which segment kinetics are allowed to depend on $\operatorname{tr}\boldsymbol{\tau}_j$ is the Phan-Thien–Tanner model[8] which was discussed previously in connection with non-affine segment motion. Phan-Thien and Tanner assume that both the creation and loss rates depend on the mean squared segment vector $\langle Q^2\rangle_j$:

$$L_j = \hat{L}_j(\langle Q^2\rangle_j)\psi_{N,\mathrm{eq}} \tag{20.5-42}$$

$$\lambda_j = \lambda_j(\langle Q^2\rangle_j) \tag{20.5-43}$$

The constitutive equation and pressure are then given by Eqs., 20.5-28, 29, 42, and 43. To evaluate $\langle Q^2\rangle_j$ we note that since $\boldsymbol{\pi}_j = -H_N\langle \boldsymbol{QQ}\rangle_j$ we must have

$$\langle Q^2\rangle_j = -\frac{1}{H_N}\operatorname{tr}\boldsymbol{\pi}_j$$
$$= -\frac{1}{H_N}(\operatorname{tr}\boldsymbol{\tau}_j + 3p_j)$$
$$= (N-1)a^2\left(\hat{L}_{j,\mathrm{eq}}\lambda_{j,\mathrm{eq}} - \frac{1}{3kT}\operatorname{tr}\boldsymbol{\tau}_j\right) \tag{20.5-44}$$

The differential equation for the extra stress is Eq. 20.5-30.

[7] Acierno et al., *op. cit.*

[8] N. Phan-Thien and R. I. Tanner, *J. Non-Newtonian Fluid Mech.*, **2**, 353–365 (1977); N. Phan-Thien, *J. Rheol.*, **22**, 259–283 (1978); R. I. Tanner, *J. Non-Newtonian Fluid Mech.*, **5**, 103–112 (1979).

To simplify Eq. 20.5-30 we next assume that λ_j^{-1} and $\hat{L}_j$ both have the same dependence on tr τ_j. We write this as

$$\hat{L}_j(\text{tr } \tau_j) = \frac{G_0}{kT\lambda_j(\text{tr } \tau_j)} \tag{20.5-45}$$

where G_0 is a constant modulus. It then follows that

$$\hat{L}_{j,\text{eq}}\lambda_{j,\text{eq}} = \hat{L}_j\lambda_j = \frac{G_0}{kT} \tag{20.5-46}$$

so that the extra stress is given by[9]

$$\tau_j + \lambda_j(\text{tr } \tau_j)\tau_{j(1)} = -G_0\lambda_j(\text{tr } \tau_j)\dot{\gamma} \tag{20.5-47}$$

Finally, we let

$$\lambda_j = \frac{\lambda_{j0}}{Y(\text{tr } \tau_j)} \tag{20.5-48}$$

where λ_{j0} is a constant with units of time and Y is a dimensionless function of τ_j. The same function Y is used for all j. The constitutive equation then becomes

$$Y(\text{tr } \tau_j)\tau_j + \lambda_{j0}\tau_{j(1)} = -\eta_j\dot{\gamma} \tag{20.5-49}$$

where $\eta_j = G_0\lambda_{j0}$. Finally, in the Phan-Thien–Tanner model, the segment kinetics that lead to Eq. 20.5-49 are combined with the non-affine motion assumption that leads to Eq. 20.5-10. In this way we obtain

$$\tau = \sum_j \tau_j \tag{20.5-50}$$

$$Y(\text{tr } \tau_j)\tau_j + \lambda_{j0}\tau_{j(1)} + \tfrac{1}{2}\lambda_{j0}\xi\{\dot{\gamma}\cdot\tau_j + \tau_j\cdot\dot{\gamma}\} = -\hat{\eta}_j\dot{\gamma} \tag{20.5-51}$$

$\hat{\eta}_j$ being given by Eq. 20.5-11. To complete the model an expression for Y must be postulated. Phan-Thien and Tanner have suggested two empirical forms

$$Y = \begin{cases} 1 - \varepsilon\lambda_{j0}(\text{tr } \tau_j)/\hat{\eta}_j & \text{(20.5-52a)} \\ \exp(-\varepsilon\lambda_{j0}(\text{tr } \tau_j)/\hat{\eta}_j) & \text{(20.5-52b)} \end{cases}$$

in which $\varepsilon \geq 0$ is an adjustable constant. The difference in the choice of Y can be seen in the elongational viscosity. For Eq. 20.5-52a, $\bar{\eta}$ is a monotone increasing function of $\dot{\varepsilon}$ which approaches a constant value as $\dot{\varepsilon} \to \infty$. For Eq. 20.5-52b, $\bar{\eta}$ goes through a maximum with increasing $\dot{\varepsilon}$.

[9] Note that Eq. 20.5-47 is very similar to the White–Metzner model, Eq. 7.3-1. The difference is that in the Phan-Thien and Tanner model the time constant is allowed to depend on tr τ whereas in the White Metzner model the time constant depends on $\dot{\gamma}$.

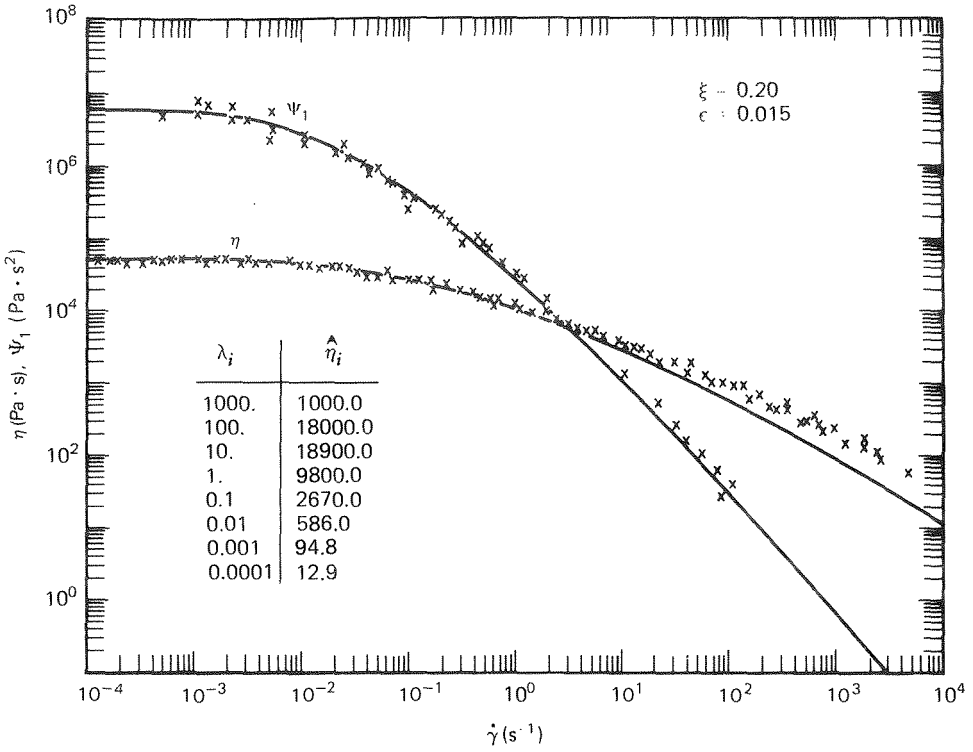

FIGURE 20.5-1. Comparison of predictions of the Phan-Thien Tanner model, Eqs. 20.5-50, 51 and 52b, with η and Ψ_1 data for a low density polyethylene melt. The constants λ_{0j} and $\hat{\eta}_j$ were fit with linear viscoelastic data (cf. Example 5.3-7); the constants ξ and ε were chosen to be 0.2 and 0.015, respectively, in order to achieve a best fit of the data. Data from H. M. Laun, *Rheol. Acta*, **17**, 1-15 (1978).

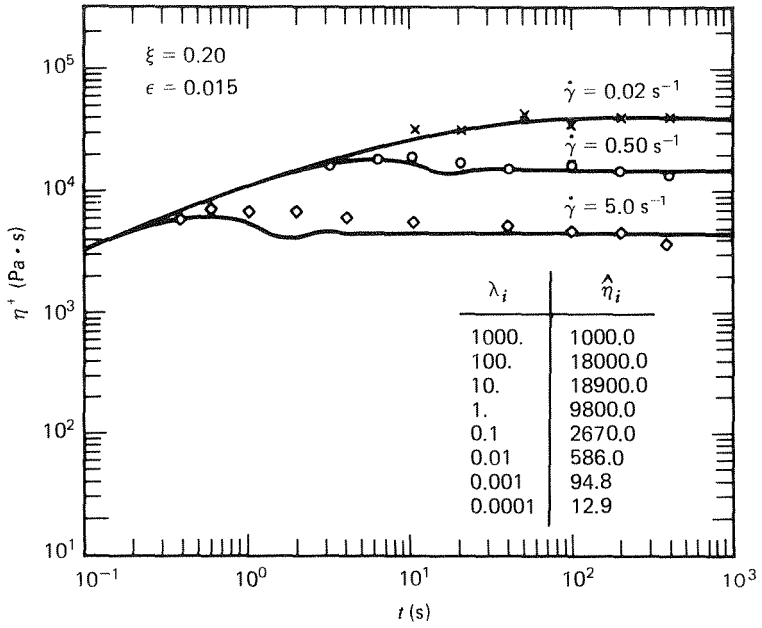

FIGURE 20.5-2. Comparison of the Phan-Thien Tanner model predictions with low density polyethylene data for η^+ in the start-up of steady shear flow. The model parameters are the same as in Fig. 20.5-1. Data as reported by M. H. Wagner, *Rheol. Acta*, **15**, 136-142 (1976).

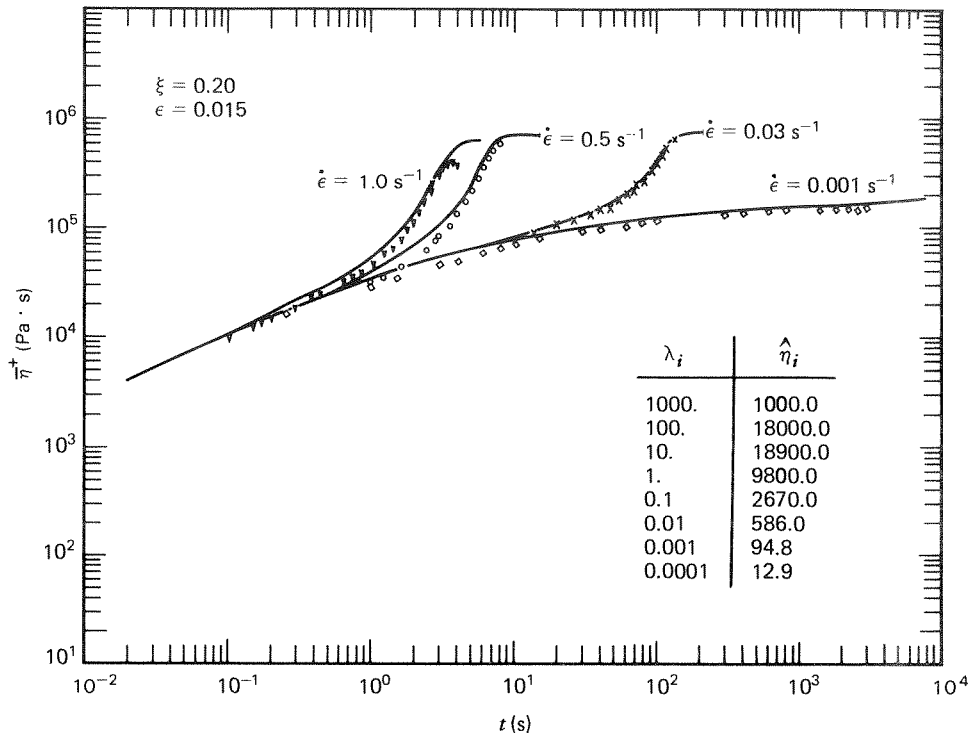

FIGURE 20.5-3. Comparison of the Phan-Thien-Tanner model predictions with low density polyethylene data for $\bar{\eta}^+$ in the start-up of steady elongational flow. The model parameters are the same as in Fig. 20.5-1. Data as reported by M. H. Wagner, *Rheol. Acta*, **18**, 39-50 (1979).

A comparison of the Phan-Thien-Tanner model (with Y given by Eq. 20.5-52b) predictions with rheological properties of low density polyethylene is shown in Figs. 20.5-1 to 3. In making these fits, the linear viscoelastic properties η' and η'' were first used to determine the λ_{j0} and $\hat{\eta}_j$. This procedure is illustrated in Example 5.3-7 and the values for λ_{j0} and $\hat{\eta}_j$ are those given in Table 5.3-7 (in this table λ_{j0} is listed as λ_j). After the λ_{j0} and $\hat{\eta}_j$ are determined, there are only two adjustable constants, ξ and ε, to be used in fitting nonlinear material functions. The choices of $\xi = 0.015$ and $\varepsilon = 0.2$ used here represent best fits of the low-density polyethylene data. In fitting these parameters it is found that the shear-flow properties are insensitive to ε and the shearfree flow properties are insensitive to ξ. Thus ξ and ε can be determined from separate sets of experiments. The fits are seen to be quite good, although it is not possible to fit exactly both η and Ψ_1 in the high shear rate region with the same value of ξ.

Wagner Model

An even more successful equation of the form of Eqs. 20.5-32 and 33 for describing rheological properties of molten polymers is one in which the memory function includes a scalar function of strain between times t' and t as a factor. Step-strain experiments[10] (cf.

[10] H. M. Laun, *Rheol. Acta*, **17**, 1-15 (1978); Y. Einaga, K. Osaki, M. Kurata, and M. Tamura, *Polymer J.*, **2**, 550-552 (1971).

Figs. 3.4-15 and 16) have given compelling evidence for such a "strain/time" factorization, at least in the terminal zone of the relaxation spectrum.

Wagner[11] assumes that the creation rates $\hat{L}_j$ are constant and that there are two *independent* mechanisms for segment loss:

(1) one, due to Brownian motion, as described by constant loss probabilities $1/\lambda_j$, and

(2) another, due to "rupture by deformation." For this mechanism, the probability that a segment will survive from the instant of creation t' to the present time t is the same for all segments and is denoted by $1/\lambda_d(t', t)$.

Since the two loss mechanisms are independent, the total loss probability $1/\lambda_j(t', t)$ is given

$$\frac{1}{\lambda_j(t', t)} = \frac{1}{\lambda_j} + \frac{1}{\lambda_d(t', t)} \tag{20.5-53}$$

The molecular weight and temperature dependence of λ_j and $\hat{L}_j$ are the same as for the Lodge network model, Eqs. 20.4-14 and 15. The deformation dependent term $\lambda_d(t', t)$ is independent of molecular weight and temperature.

The constitutive equation is then given by Eqs. 20.5-31 and 32 with

$$\begin{aligned} M(t, t') &= kT \sum_j \hat{L}_j e^{-(t-t')/\lambda_j} \exp\left(- \int_{t'}^{t} \frac{1}{\lambda_d(t'', t)}\, dt'' \right) \\ &= kTh(I_w(t', t)) \sum_j \hat{L}_j e^{-(t-t')/\lambda_j} \end{aligned} \tag{20.5-54}$$

in which the *damping function* h is defined by

$$h(I_w(t', t)) = \exp\left(- \int_{t'}^{t} \frac{1}{\lambda_d(t'', t)}\, dt'' \right) \tag{20.5-55}$$

I_w is a generalized strain invariant, formed from the first and second invariants of $\mathbf{B}$ (cf. Eqs. 8.3-1 and 2)

$$\begin{aligned} I_1 &= \text{tr } \mathbf{B} \\ I_2 &= \text{tr } \mathbf{B}^{-1} \end{aligned} \tag{20.5-56}$$

The specific dependence of I_w on I_1 and I_2 is determined empirically.

For small strains it is assumed that no segments are broken by the deformation, so that $\lambda_d \to \infty$ and $h \to 1$. Thus the constants $\hat{L}_j$ ($\equiv \eta_j/kT\lambda_j^2$) and λ_j can be determined from linear viscoelastic data in the same way as for the Lodge network model. The damping function h was fit by Wagner to stress relaxation data for single-step, shear strain experiments and stress growth data in the start-up of steady elongational flow experiments for a low density polyethylene melt. This led to the following form for h

$$h = \exp\left[-\beta\sqrt{\alpha I_1 + (1-\alpha) I_2 - 3} \right] \tag{20.5-57}$$

[11] M. H. Wagner, *Rheol. Acta*, **18**, 33-50 (1979).

with $\beta = 0.18$ and $\alpha = 0.032$. Note that h in Eq. 20.5-57 is equivalent to a deformation loss probability

$$\frac{1}{\lambda_d(t', t)} = -\frac{\beta}{2\sqrt{I_w}} \frac{dI_w}{dt'} \tag{20.5-58}$$

where

$$I_w = \alpha I_1 + (1 - \alpha) I_2 - 3 \tag{20.5-59}$$

The resulting constitutive equation, a particular case of the Rivlin–Sawyers class of equations, gives an excellent description of a variety of experiments in shear and elongation, but it significantly overestimates the free recovery following elongation at constant rates.[12] The agreement with shear recovery data (following shear flow) is satisfactory, however.

To remedy the errors in free recovery following start-up of steady elongational flow, Wagner and Stephenson[13] revised the second mechanism for segment loss as follows:

(2′) Segments are lost *irreversibly* during a nondecreasing deformation and are not recreated during subsequent decreasing deformation; the deformation-dependent survival function h in Eq. 20.5-54 should be replaced by a functional H of strain given by

$$H(t, t') = \underset{t''=t'}{\overset{t''=t}{\text{Min}}} \{h(I_w(t', t''))\} \tag{20.5-60}$$

where "Min" denotes the minimum value assumed by the function h over the interval indicated.

The terms decreasing and non-decreasing as applied to the deformations here are defined by

$$\text{A deformation is } \left\{\begin{matrix}\text{non-decreasing}\\ \text{decreasing}\end{matrix}\right\} \text{ throughout an interval } (t', t) \text{ where } t' < t$$

$$\text{provided that } h(I_w(t', t'')) \text{ is } \left\{\begin{matrix}\text{increasing}\\ \text{non-increasing}\end{matrix}\right\} \text{ for } t' < t'' < t \tag{20.5-61}$$

With these modifications, network segments that are lost during elongation from deformation-induced rupture are not recreated during recovery. Much better agreement with recovery data following elongation is then obtained.

An interesting consequence of the appearance of two times in $\lambda_j(t', t)$ in the Wagner model is that it is not in general possible to find an equivalent differential form for the constitutive equation, as we have been able to do for the other network models discussed in this chapter. A further discussion of the Wagner model and its material functions is given in Example 8.3-2.

[12] M. H. Wagner, *I. U. T. A. M. Conf.*, Louvain, Belgium (1978).
[13] M. H. Wagner and S. E. Stephenson, *J. Rheol.*, **23**, 491–504 (1979).

PROBLEMS

20A.1 Elongation of a Rubber Band

A slender rubber band has an equilibrium length of 0.60 m. One end of the rubber band is held fixed, while a weight of mass 0.050 kg is attached to the other end. Under this weight the rubber band is stretched to a total length of 0.80 m. Assume that the rubber is a neo-Hookean material, and calculate the weight necessary to stretch the rubber band to 1.00 m.

20A.2 Determination of Parameters in the Mooney Equation

A rectangular strip of crosslinked rubber sheet has equilibrium dimensions given by $x_0 = 0.30$ m, $y_0 = 0.02$ m, and $z_0 = 0.001$ m (Fig. 20A.2). A first test is performed on the sample by applying tensile forces of 10 N parallel to the x-axis to the ends of the material that are initially located at $x = 0$ and $x = x_0$. Under the action of this load, the strip undergoes a homogeneous elongation that increases its length by 71% in the x-direction. The material is then allowed to return to its equilibrium shape. A second experiment is then performed by clamping the edges at $y = 0$ and $y = y_0$; in this way the dimension of the strip in the x-direction is held fixed at x_0. Tensile forces of 50 N are now applied to the sample parallel to the y-axis by means of the clamps, and the strip undergoes homogeneous pure shear that increases its y-dimension by 12%. Assume that the rubber is described by the Mooney equation given in Eq. 20.3-15, and estimate the modulus G_0 and the parameter q.

20B.1 Estimation of Segment Number Density

Consider the elementary network model for a macromolecular fluid described in §20.4. Assume that there is only one kind of segment.

a. Show that the total number density of segments is given as follows in terms of the viscometric functions.

$$n = \frac{2[\eta(\dot{\gamma})]^2}{kT\Psi_1(\dot{\gamma})} \tag{20B.1-1}$$

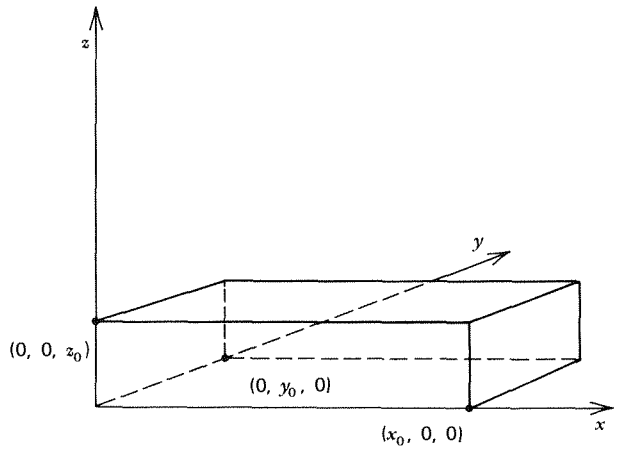

FIGURE 20A.2. A rectangular strip of rubber sheet with dimensions $x_0 = 0.30$ m, $y_0 = 0.02$ m, and $z_0 = 0.001$ m.

b. From the data[1] in Figs. 3.3-3 and 5 plot $2[\eta(\dot{\gamma})]^2/kT\Psi_1(\dot{\gamma})$ as a function of the shear rate $\dot{\gamma}$ for the 1.5% polyacrylamide solution.

c. Use Eq. 20B.1-1 and the plot to make a rough estimate of the total number density of segments in the solution. Are the data consistent with the theory?

20B.2 Strain Increment Test of a Network Model[2]

It is desired to test whether a given polymer material can be described by the generalization of the Lodge network model, Eq. 20.5-32, in which $M(t, t')$ is allowed to be any scalar functional of the deformation history. Specifically consider a shear flow that is arbitrary up to a certain time t_0. Let x', y', z' denote the past coordinates of a typical particle that just prior to time t_0 has coordinates x^-, y^-, z^-. Then at time t_0 an additional shear strain γ_0 is imposed on the material. Denote the new coordinates of the particle by x^+, y^+, z^+. In other words we consider the following deformation history:

For $t < t_0^-$:

$$x = x' - \gamma_{yx}(t, t')y' \qquad y = y' \qquad z = z' \tag{20B.2-1}$$

For $t = t_0^+$:

$$x^+ = x' + (\gamma_0 - \gamma_{yx}(t_0^-, t'))y' \qquad y^+ = y' \qquad z^+ = z' \tag{20B.2-2}$$

where $\gamma_{yx}(t, t') = \int_t^{t'} \dot{\gamma}_{yx}(t'')dt''$ is the shear strain from time t to time t'. Note that $\gamma_0 = -\int_{t_0^-}^{t_0^+} \dot{\gamma}_{yx}(t'')dt''$.

a. Assume that M is unchanged by the instantaneous deformation at time t_0, and derive expressions for τ_{yx}^-, $(\tau_{xx} - \tau_{yy})^-$, τ_{yx}^+, and $(\tau_{xx} - \tau_{yy})^+$ where the superscripts "$-$" and "$+$" indicate that the stress-tensor components are to be evaluated just prior to and just after the instantaneous deformation, respectively.

b. Let n denote the total number density of segments at time t_0. By using the results of Problem 20B.5 for $\dot{n}_j(t, t')$ and Eq. 20.4-30, show that

$$\tau_{yx}^+ = \tau_{yx}^- - nkT\gamma_0 \tag{20B.2-3}$$

$$(\tau_{xx} - \tau_{yy})^+ = (\tau_{xx} - \tau_{yy})^- + \gamma_0(\tau_{yx}^+ + \tau_{yx}^-) \tag{20B.2-4}$$

Equations 20B.2-3 and 4 combined represent a test (albeit not a sufficient condition) of the validity of the assumptions leading to Eq. 20.5-32, as well as a method for estimating the number density of segments n in any shear flow experiment.

20B.3 Start-Up of Shear Flow of the Lodge Network Model

Consider the constitutive equation given by Eq. 20.4-11 in which the memory function M is a function of $(t - t')$ only.

a. Derive expressions for the growth functions η^+, Ψ_1^+, and Ψ_2^+ in terms of $M(t - t')$.

[1] J. D. Huppler, E. Ashare, and L. A. Holmes, *Trans. Soc., Rheol.*, **11**, 159–179 (1967).

[2] A. S. Lodge and J. Meissner, *Rheol. Acta*, **11**, 351–352 (1972).

b. From the expressions for η^+ and Ψ_1^+ show that:

$$\Psi_1^+(t, \dot{\gamma}) = 2\left[t\eta^+(t, \dot{\gamma}) - \int_0^t \eta^+(t', \dot{\gamma})dt'\right] \tag{20B.3-1}$$

c. Derive expressions for η^+, Ψ_1^+, and Ψ_2^+ corresponding to the memory function M given in Eq. 20.4-11.

Answer: c. $\eta^+ = \sum_j \eta_j[1 - e^{-t/\lambda_j}]$

$$\Psi_1^+ = 2\sum_j \eta_j\lambda_j[1 - (1 + t/\lambda_j)e^{-t/\lambda_j}]$$

$$\Psi_2^+ = 0$$

20B.4 Verification of the Distribution Function Obtained from the Network Theory for Solids

a. Show that Eq. 20.2-23 is the correct distribution function for a network solid by substituting it into the convection equation.

b. By taking the convected derivative of Eq. 20.3-12, show that Eq. 20.3-13 is the differential form of the constitutive equation for a macromolecular network solid.

20B.5 Alternative Form for the Fluid Network Model Constitutive Equation

It is desired to rewrite the constitutive equation for the network model for polymeric fluids given in Eqs. 20.5-31 through 33 in terms of the number density of segments. By paralleling the development that led to Eq. 20.4-29, but allowing for time-dependent segment creation and loss rates, show that the memory function in Eq. 20.5-33 can be written as

$$M(t, t') = \sum_j \dot{n}_j(t, t')kT \tag{20B.5-1}$$

where $\dot{n}_j(t, t')$ is defined in Eq. 20.4-21.

20C.1 Constrained Recoil after Steady Shear Flow of the Lodge Rubberlike Liquid[3]

Consider a fluid described by the constitutive equation given by Eq. 20.4-11 with the assumption that the memory function, M, is a function of $t - t'$ only. The fluid is contained between two parallel plates, and has prior to time $t = 0$ been undergoing a steady shear flow with shear rate $\dot{\gamma}_0$. At time $t = 0$ the shear stress is suddenly removed. The fluid then recoils, and the magnitude of shear from time $t = 0$ is designated by $\gamma(t) = \int_0^t \dot{\gamma}(t'')dt''$. It is assumed that inertial effects are negligible and that the flow during recoil is homogeneous.

a. Show that for time $t \geq 0$ the magnitude of shear satisfies the integral equation:

$$M_0\gamma(t) + \dot{\gamma}_0\int_t^\infty M(s)(t - s)ds = \int_0^t M(t - s)\gamma(s)ds \tag{20C.1-1}$$

Here and in the following we use the notation:

$$M_r = \int_0^\infty M(s)s^r\, ds \tag{20C.1-2}$$

[3] A. S. Lodge, *Elastic Liquids*, Academic Press, New York (1964), pp. 144–147. See also Examples 6.2-5 and 6.3-2.

b. From Eq. 20C.1-1 show that the "instantaneous recoil," that is $\gamma_0 = \lim_{t \to 0-} \gamma(t)$, is given by:

$$\gamma_0 = \frac{\dot{\gamma}_0 M_1}{M_0} \tag{20C.1-3}$$

c. Take the Laplace transform of Eq. 20C.1-1 by using the convolution theorem. Show that the Laplace transform $\bar{\gamma}(p)$ of $\gamma(t)$ is given by

$$\bar{\gamma}(p) = \dot{\gamma}_0 \frac{M_0 p^{-2} - M_1 p^{-1} - \bar{M}(p) p^{-2}}{\bar{M}(p) - M_0} \tag{20C.1-4}$$

where $\bar{M}(p)$ is the Laplace transform of $M(s)$.

d. Expand $\bar{M}(p)$ in powers of p, and use the final value theorem to show that the "ultimate recoil," that is, $\gamma_\infty = \lim_{t \to \infty} \gamma(t)$ is given by

$$\gamma_\infty = \dot{\gamma}_0 \frac{M_2}{2M_1} \tag{20C.1-5}$$

e. Discuss a form of $M(s)$ for which $\gamma_\infty = \gamma_0$ and a form for which $\gamma_\infty > \gamma_0$.

20C.2 Rapid Deformations of the Lodge Rubberlike Liquid[4]

Consider a network model given by Eq. 20.4-11, where M is a function of $t - t'$ only and is continuous at $t' = t$. The liquid has been undergoing an arbitrary homogeneous deformation at constant volume up to a time t_1. The position vector of a typical particle P at time t_1 is designated by $\boldsymbol{r}_1$. Similarly at a past time t' the position vector of P is designated by $\boldsymbol{r}'$.

a. At time t_1 the stress is suddenly made isotropic, and the liquid "instantaneously" undegoes a homogeneous deformation at constant volume, such that the position vector of P is given by $\boldsymbol{r}_0$. Show that the position vector $\boldsymbol{r}_0$ satisfies the following equations:

$$G_0 \left(\frac{\partial}{\partial \boldsymbol{r}_0} \boldsymbol{r}_1\right) \cdot \left(\frac{\partial}{\partial \boldsymbol{r}_0} \boldsymbol{r}_1\right)^\dagger = \int_{-\infty}^{t_1} M(t_1 - t') \left(\frac{\partial}{\partial \boldsymbol{r}'} \boldsymbol{r}_1\right) \cdot \left(\frac{\partial}{\partial \boldsymbol{r}'} \boldsymbol{r}_1\right)^\dagger dt' \tag{20C.2-1}$$

$$\det\left\{\left(\frac{\partial}{\partial \boldsymbol{r}_0} \boldsymbol{r}_1\right) \cdot \left(\frac{\partial}{\partial \boldsymbol{r}_0} \boldsymbol{r}_1\right)^\dagger\right\} = 1 \tag{20C.2-2}$$

Here G_0 is a constant that depends on the deformation history up to time t_1 as given by Eq. 20C.2-1.

b. Instead of the deformation described under part a, we now assume that at time t_1 the liquid is suddenly subjected to an arbitrary, rapid, homogeneous deformation at constant volume to a state t. Show that for such rapid deformations, the liquid model behaves as a solid described by:

$$\tau(t) = G_0 \gamma_{[0]}(t, t_0) \tag{20C.2-3}$$

The modulus G_0 and the isotropic stress state t_0 are those determined by Eqs. 20C.2-1 and 2. That is for rapid deformations the Lodge network model behaves as a neo-Hookean solid with modulus and isotropic stress state determined by the past history of deformation.

[4] This problem is patterned after the development by A. S. Lodge, *Elastic Liquids*, Academic Press, New York (1964), pp. 124–129.

20C.3 Free Recovery after Steady-Shear Flow of the Lodge Rubberlike Liquid[5]

Consider the network model given by Eqs. 20.4-11, in which M is taken to be a function of $t - t'$ only. Assume that the liquid model has been undergoing a steady shear flow of shear rate $\dot{\gamma}_0$ up to time $t = t_1$. Then the stress is suddenly made isotropic. The subsequent deformation of the liquid is called a free recovery. For the present model the free recovery consists of an "instantaneous recovery" and a time-dependent "delayed recovery." During the delayed recovery the fluid slowly settles to an equilibrium shape. It is desired to use the results of Problem 20C.2 part (**a**) to calculate the instantaneous recovery.

Introduce a rectangular Cartesian coordinate system, such that the steady shear flow is given by $v_1 = \dot{\gamma}_0 x_2$, $v_2 = 0$, and $v_3 = 0$. For purposes of computation we assume that the instantaneous recovery may be decomposed artificially as follows:

First, imagine a shearfree deformation in which a typical particle P changes position vector from $\boldsymbol{r}_1$ to $\tilde{\boldsymbol{r}}$, such that

$$\tilde{\boldsymbol{r}} = [\boldsymbol{\Lambda}_1 \cdot \boldsymbol{r}_1] \tag{20C.3-1}$$

where

$$\boldsymbol{\Lambda}_1 = \begin{pmatrix} \alpha_1 & 0 & 0 \\ 0 & \alpha_2 & 0 \\ 0 & 0 & \alpha_3 \end{pmatrix} \tag{20C.3-2}$$

Then imagine a shear flow in which P further changes position vector from $\tilde{\boldsymbol{r}}$ to the position $\boldsymbol{r}_0$ in the state after the instantaneous recovery, such that

$$\boldsymbol{r}_0 = [\boldsymbol{\Lambda}_2 \cdot \tilde{\boldsymbol{r}}] \tag{20C.3-3}$$

where

$$\boldsymbol{\Lambda}_2 = \begin{pmatrix} 1 & -\gamma & 0 \\ 0 & 1 & 0 \\ 0 & 0 & 1 \end{pmatrix} \tag{20C.3-4}$$

a. Show that

$$\alpha_2 = \alpha_3 = \alpha_1^{-1/2} = \alpha \tag{20C.3-5}$$

$$\alpha = [1 + \dot{\gamma}_0^2(M_0 M_2 - M_1^2)/M_0^2]^{1/6} \tag{20C.3-6}$$

$$\gamma = \dot{\gamma}_0 M_1/(M_0 \alpha^3) \tag{20C.3-7}$$

$$G_0 = M_0 \alpha^2 \tag{20C.3-8}$$

$$\alpha \geq 1 \tag{20C.3-9}$$

Here G_0 is the modulus defined by Eq. 20C.2-1 and the M_r are constants defined by Eq. 20C.1-2.

[5] This problem is patterned after the development by A. S. Lodge, *Elastic Liquids*, Academic Press, New York (1964), pp. 131–139.

b. Show that the results of the above analysis alternatively may be expressed by the following statements concerning instantaneous recovery following shear flow of the Lodge network model:

1. The separation of each pair of material shearing planes increases by the factor α given above.
2. Each material line in the shearing planes, perpendicular to the direction of shear, increases in length by the factor α.
3. Each material line in the shearing planes, parallel to the direction of shear, is contracted by a factor of α^2.
4. Each material line that is normal to the shearing planes just prior to the moment of recovery is tilted backwards with respect to the original shear direction through an angle ε where $\tan \varepsilon = \gamma$ and γ is given above.

c. For a memory function of the form

$$M(s) = \frac{\eta}{\lambda^2} e^{-s/\lambda} \tag{20C.3-10}$$

show that

$$\alpha = [1 + (\lambda \dot{\gamma}_0)^2]^{1/6} \tag{20C.3-11}$$

$$\tan \varepsilon = \gamma = (\lambda \dot{\gamma}_0)[1 + (\lambda \dot{\gamma}_0)^2]^{-1/2} \tag{20C.3-12}$$

$$\frac{\lambda G_0}{\eta} = [1 + (\lambda \dot{\gamma}_0)^2]^{1/3} \tag{20C.3-13}$$

Here G_0 is the modulus given by Eq. 20C.2-1. Prepare plots to show α, $\tan \varepsilon$ and $\lambda G_0/\eta$ as functions of $\lambda \dot{\gamma}_0$.

20D.1 General Solution to the Convection Equation[6]

Assume that the loss probability λ_{iN} is a function of time alone, that is λ_{iN} is independent of $\boldsymbol{Q}$. Show that the convection equation, Eq. 20.2-7, is satisfied by

$$\Psi_{iN} = \int_{-\infty}^{t} \exp\left(\int_{t}^{t'} \lambda_{iN}^{-1}(t'')\, dt''\right) L_{iN}(\boldsymbol{\Delta}(t, t') \cdot \boldsymbol{Q}, t') dt' \tag{20D.1-1}$$

where L_{iN} depends on $[\boldsymbol{\Delta} \cdot \boldsymbol{Q}]$ as well as on t'.

[6] This problem is due to J. M. Wiest (personal communication).